Preclinical modeling of metabolic syndrome to study the pleiotropic effects of novel antidiabetic therapy independent of obesity

Jonathan P Mochel, Jessica L Ward, Thomas Blondel, Debosmita Kundu, Maria M Merodio, Claudine Zemirline, Emilie Guillot, Ryland T Giebelhaus, Paulina de la Mata, Chelsea A Iennarella-Servantez, et al.

scientific reports

Check for updates

OPEN

Preclinical modeling of metabolic syndrome to study the pleiotropic effects of novel antidiabetic therapy independent of obesity

Jonathan P. Mochel[1,2]✉, Jessica L. Ward[3], Thomas Blondel[4], Debosmita Kundu[2], Maria M. Merodio[3], Claudine Zemirline[4], Emilie Guillot[4], Ryland T. Giebelhaus[5], Paulina de la Mata[5], Chelsea A. Iennarella-Servantez[2], April Blong[3], Seo Lin Nam[5], James J. Harynuk[5], Jan Suchodolski[6], Asta Tvarijonaviciute[7], José Joaquín Cerón[7], Agnes Bourgois-Mochel[1,2], Faiez Zannad[8], Naveed Sattar[9] & Karin Allenspach[1,2]

Cardiovascular-kidney-metabolic health reflects the interactions between metabolic risk factors, chronic kidney disease, and the cardiovascular system. A growing body of literature suggests that metabolic syndrome (*MetS*) in individuals of normal weight is associated with a high prevalence of cardiovascular diseases and an increased mortality. The aim of this study was to establish a non-invasive preclinical model of *MetS* in support of future research focusing on the effects of novel antidiabetic therapies beyond glucose reduction, independent of obesity. Eighteen healthy adult Beagle dogs were fed an isocaloric Western diet (WD) for ten weeks. Biospecimens were collected at baseline (*BAS1*) and after ten weeks of WD feeding (*BAS2*) for measurement of blood pressure (BP), serum chemistry, lipoprotein profiling, blood glucose, glucagon, insulin secretion, NT-proBNP, angiotensins, oxidative stress biomarkers, serum, urine, and fecal metabolomics. Differences between *BAS1* and *BAS2* were analyzed using non-parametric Wilcoxon signed-rank testing. The isocaloric WD model induced significant variations in several markers of *MetS*, including elevated BP, increased glucose concentrations, and reduced HDL-cholesterol. It also caused an increase in circulating NT-proBNP levels, a decrease in serum bicarbonate, and significant changes in general metabolism, lipids, and biogenic amines. Short-term, isocaloric feeding with a WD in dogs replicated key biological features of *MetS* while also causing low-grade metabolic acidosis and elevating natriuretic peptides. These findings support the use of the WD canine model for studying the metabolic effects of new antidiabetic therapies independent of obesity.

Keywords Western diet, Metabolic syndrome, Cardiorenal metabolic diseases, One health

Type 2 diabetes mellitus (T2DM) is a chronic metabolic disorder characterized by hyperglycemia resulting from insulin resistance and impaired insulin secretion[1]. Recent data from the National Diabetes Statistics Report indicate that 37.3 million Americans suffer from T2DM[2]. In addition, the economic cost of diabetes and prediabetes was estimated to reach $322 billion in the U.S in 2012. Accumulating data from several large, placebo-controlled studies suggests that sodium-glucose transporter 2 (SGLT-2) inhibitors and glucagon-like

[1]Precision One Health Initiative, Department of Pathology, University of Georgia College of Veterinary Medicine, 501 D.W. Brooks Drive, Athens, GA 30602, USA. [2]SMART Pharmacology, Iowa State University, Ames, IA 50011-1250, USA. [3]Veterinary Clinical Sciences, Iowa State University, Ames, IA 50011-1250, USA. [4]Ceva Santé Animale, 33500 Libourne, France. [5]The Metabolomics Innovation Centre, Department of Chemistry, University of Alberta, T6G 2G2 Edmonton, Canada. [6]Gastrointestinal Laboratory, Texas A&M University, College Station, TX 77845, USA. [7]Interdisciplinary Laboratory of Clinical Analysis (Interlab-UMU), Veterinary School, Regional Campus of International Excellence 'Campus Mare Nostrum', University of Murcia, Campus de Espinardo s/n, Espinardo, 30100 Murcia, Spain. [8]Université de Lorraine, Centre d'Investigations Cliniques Plurithématique 1433 and Inserm U1116, CHRU Nancy, FCRIN INI-CRCT, 54000 Nancy, France. [9]School of Cardiovascular and Metabolic Health, BHF Glasgow Cardiovascular Research Centre, University of Glasgow, 126 University Place, Glasgow G12 8TA, Scotland, UK. ✉email: jpmochel@uga.edu

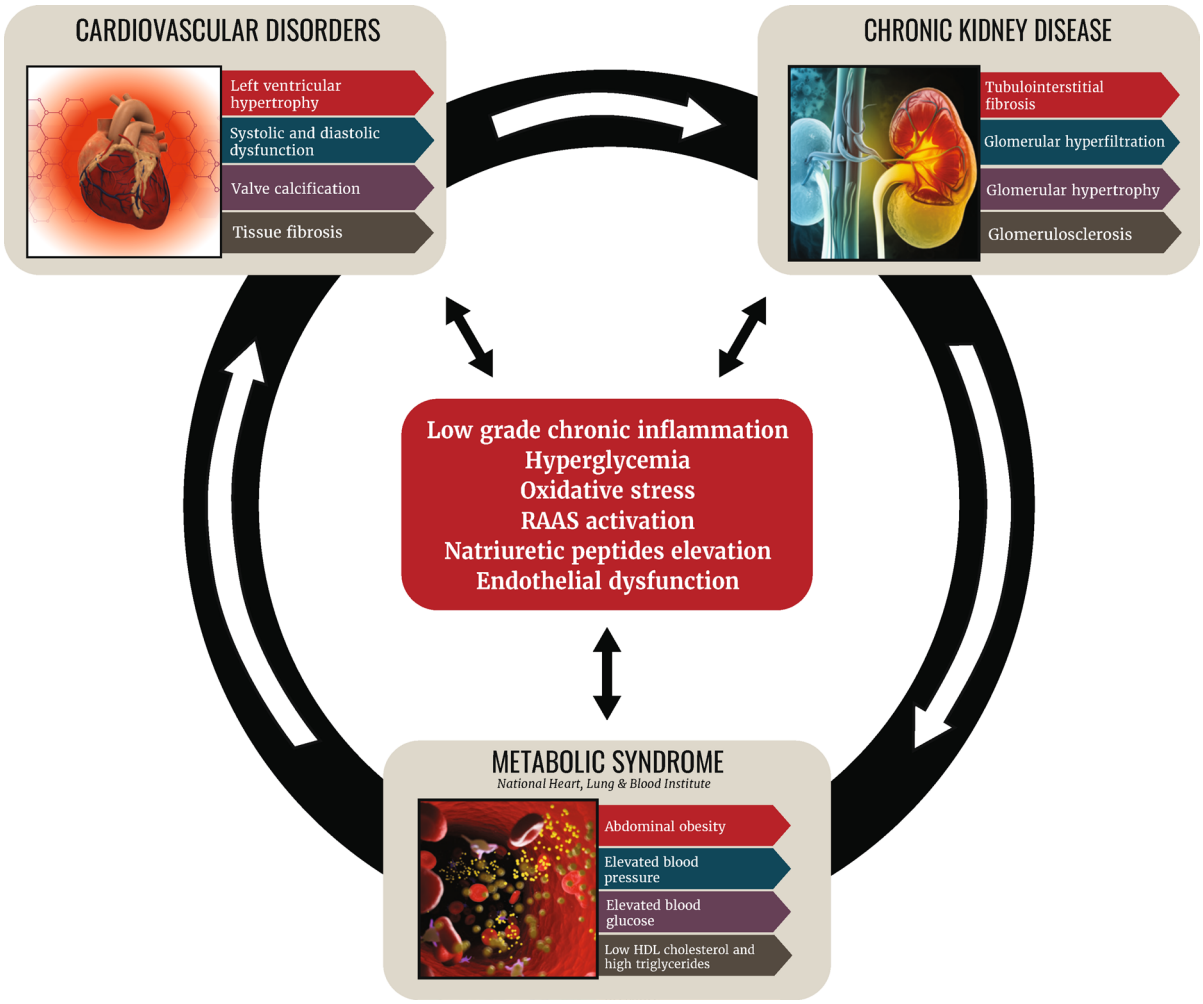

Fig. 1. Molecular bases for the interrelationship between cardiovascular, renal, and metabolic diseases. Adjusted and simplified from Kadowaki et al. [120].

peptide 1 (GLP-1) receptor agonists offer therapeutic benefits in the management of cardiovascular diseases, regardless of the patient's diabetic status[3–11]. In addition to their effects on glucose excretion, SGLT-2-inhibitors positively impact systemic metabolism by reducing inflammation and oxidative stress, shifting metabolism towards ketone body production, promoting autophagy, and suppressing glycation end-product signaling[9]. These findings align with the American Heart Association's recent definition of ***cardiovascular-kidney-metabolic health***[12], a concept which represents the interplay between metabolic disorders like T2DM, chronic kidney disease, and the cardiovascular system (Fig. 1).

The pleiotropic effects of SGLT-2 inhibitors and GLP-1 agonists provide an opportunity to target several cardiorenal metabolic disorders. ***This can be achieved experimentally using a disease model that replicates key features of metabolic syndrome*** (***MetS***), a cluster of risk factors that include obesity, dyslipidemia, hypertension, and insulin resistance. Collectively, these factors increase the risk of developing cardiorenal diseases, metabolic dysfunction-associated steatohepatitis and T2DM[9,13,14]. Implementing such a model would enable future mechanistic studies to explore the metabolic effects of novel antidiabetic therapy beyond glycemic control.

Rodent models, especially mice, are commonly used in translational research due to their cost-effectiveness, ethical considerations, and ease of genetic manipulation. However, despite their widespread use, murine models often fail to accurately mimic human diseases, limiting their translational value[15]. In a study published in the *Proceedings of the National Academy of Sciences*, Seok et al.[16] found that mouse models poorly replicate human inflammatory responses from various causes, reporting a poor correlation (R^2 between 0.0 and 0.1) between significantly altered genes in humans and their murine equivalents. Additionally, the high failure rate of drug discovery and development highlights the urgent need for more accurate animal models in preclinical research[17]. The FDA Modernization Act 2.0 further emphasizes this need by restricting the use of non-informative animal models, such as rodents, in experimental drug testing prior to clinical studies[18]. As a result, there is an increasing incentive to use more relevant animal models, such as dogs, which often better represent chronic diseases than rodents. Dogs have a larger body size, longer lifespan, and physiological similarities to humans, and they naturally develop diseases analogous to human conditions, including cardiorenal, metabolic, inflammatory, and neurodegenerative diseases[15,19–24].

Despite presenting some unique features in their lipid metabolism, such as low activity of cholesteryl ester transfer protein and an abundance of high-density lipoprotein (HDL)-bound plasma cholesterol (contributing to an athero-protective profile)[25,124], dogs have been extensively used for studying metabolic obesity, diabetes, dyslipidemia, and their response to therapeutic interventions[26]. As such, a comprehensive analysis published in the *Journal of Lipid Research* identified dogs as the second most translatable model (after non-human primates) for studying dyslipidemia and related pharmacological agents in humans, among 24 animal species, including rodents, rabbits and pigs[27].

In return, from the perspective of developing veterinary pharmaceuticals for spontaneous diseases in animals, the data generated in dogs from this study could guide the development of multiple therapeutic applications for SGLT-2 inhibitors and GLP-1 agonists in veterinary medicine, such as diabetes, congestive heart failure, or chronic kidney disease under the One Health paradigm[28–31].

Previous studies have shown that consistent overfeeding of dogs with a high-calorie Western diet (WD) can lead to ***MetS***, regardless of the diet's composition[32,33]. However, these investigations in dogs have primarily focused on the metabolic issues associated with obesity[32,34–37]. In both dogs and humans, obesity triggers an adipose tissue redistribution that results in an increase in visceral (vs. subcutaneous) fat. This shift in fat deposition is independently associated with the onset of ***MetS***. A study by Romero-Corral et al.[38] analyzing data from more than 6000 subjects showed that normal weight obesity, defined as the combination of normal body mass index (BMI) and high body fat content, was associated with a high prevalence of cardiometabolic dysregulation and cardiovascular risk factors. These findings were later supported by Shi et al.[39] in an analysis including 12,047 adults where normal-weight adults with ***MetS*** had the highest hazard ratio for mortality (1.70 [1.16–2.51]), compared with obese patients with ***MetS*** (1.30 [1.07–1.60]) and obese patients without ***MetS*** (1.08 [0.76–1.54]). Additionally, most clinical studies demonstrating therapeutic benefits from SGLT-2 inhibitors on cardiorenal outcome measures include a majority of *non*-obese patients[4,7,40–42]. A recent study by Adamson et al., published in the *European Journal of Heart Failure*, has unequivocally established that the efficacy of dapagliflozin for heart failure patients with reduced ejection fraction remains consistent regardless of their BMI[43]. ***These findings collectively support the rationale for establishing a metabolic dysfunction model that is independent of obesity to study the pharmacodynamic effects of drug candidates targeting the cardiovascular-kidney-metabolic health***.

In a preliminary study conducted by our consortium, dogs isocalorically fed a WD for a few weeks presented with elevated fasting bile acids, cholesterol, triglycerides, and blood pressure compared to control[44]. These findings suggest that short-term feeding with a WD can induce a clinical response that mimics ***MetS*** in healthy dogs. The aim of this research was to characterize the metabolic and molecular signatures associated with a high-fat, high-monosaccharide, and low-fiber isocaloric WD after ten weeks in dogs. Once established, this preclinical model can be used to assess the therapeutic benefits of novel antidiabetic therapy in the context of obesity-independent ***MetS*** and pave the way for translational studies that could benefit both human and veterinary medicine.

Methods

Animals

Experimental procedures were approved by the Institutional Animal Care and Use Committee at Iowa State University (Protocol Number: 21-164). All methods were performed in accordance with the relevant guidelines and regulations at Iowa State University. The authors complied with ARRIVE guidelines in the completion of this study. The study population consisted of 18 neutered young adult laboratory Beagles (9 males and 9 females, aged 12–15 months) weighing between 7.5 and 11.5 kg. They originated from a colony that had been previously acclimatized to handling and blood sampling procedures. Prior to inclusion, each dog was assessed for its general health and condition with a physical examination and had received appropriate vaccinations and deworming treatments. Normal cardiovascular structure and function were confirmed through an echocardiogram performed prior to acclimation to the study facility. No dog had received topical or systemic medications within the 28 days preceding inclusion. Each animal was assigned a unique 4-letter ear tattoo for identification purposes. Throughout the in-life phase, daily evaluations of the animals' general health and behavior were conducted by the study veterinarian (Dr. Agnes Bourgois-Mochel). Body weight and body condition scores (BCS, recorded as "underweight" vs. "ideal" vs. "overweight") were recorded weekly using the body condition system developed at the Nestle Purina Pet Care Center[45]. Detailed information on the canine body condition system can be found at: https://www.purinainstitute.com/centresquare/nutritional-and-clinical-assessments/canine-body-condition-system-sheet. All observations, including any adverse events and study interventions were systematically recorded in the raw data file.

Housing

The study animals were acclimatized to the facility for one week before the start of the study. Housing conditions were strictly in accordance with the requirements set by the United States Department of Agriculture. Each dog was housed in a 16-square foot kennel (dimensions: 4′ × 4′) with an interconnecting door, allowing for the co-housing of two animals. However, individual separation was implemented during specific periods, such as feeding times, or when necessary for specific interventions or observations.

The lighting schedule was kept from 6 a.m. to 6 p.m. The ambient temperature within the housing facilities was consistently set to 70 F (21.1 °C), with continuous monitoring. Throughout the study, the recorded temperature varied minimally, with the range extending from 67 F (19.4 °C) to 72 F (22.2 °C). Relative humidity was also closely monitored, with values fluctuating between 34 and 45%. The dogs were provided with unrestricted access to tap water, delivered via individual nipple water feeders.

Experimental design

To replicate the dietary intake of an average American diet, dogs were fed a high-fat, high-monosaccharide, low-fiber WD adjusted from parameters of the National Health and Nutrition Examination Survey (NHANES 2015–2016: Males and Females over 20 years)[46] for ten weeks. Dogs were fed isocalorically based on individually calculated metabolizable energy needs. Blood samples were collected at baseline (***BAS1***) when dogs were fed their regular diet, and then again after ten weeks of WD feeding (***BAS2***).

Diet composition for BAS1 measurements

Dogs were fed a daily diet of Royal Canin® Beagle Adult dry food (12% fat content), once in the morning, around 9 a.m. The portion size for each dog was individually calculated based on weight and resting energy requirements (RER) calculated by multiplying the animal's body weight (BW) in kilograms raised to the 0.75 power by 70: $RER = 70 \times (BW)^{0.75}$ (Eq 0.1). Any leftover was weighed and recorded in the raw data file. Nutritional information on the Royal Canin® Beagle Adult dry food is presented in Table 1.

Diet composition for BAS2 measurements

Western diets were formulated to model the average intake of American subjects over 20 years from the NHANES and were fed to meet the energy and National Research Council[47] requirements for adult dogs. Diets were home cooked and prepared in batch (N = 18 dogs) on a weekly basis, then stored frozen. Ingredients were purchased from the same supplier and brand to ensure consistency. Food was offered once daily in the morning, around 9 a.m. In cases where the provided meal was not entirely consumed, the remaining portion was carefully weighed and documented in the raw data file. The exact composition of the WD can be found in Table 2.

Sample collection

- Blood samples were drawn using a jugular catheter whenever possible, or from the saphenous or cephalic veins with single use needles. Blood samples were collected at baseline (***BAS1***) when dogs were fed their regular diet, and then again after ten weeks of WD feeding (***BAS2***) for measurement of:
    - Complete blood count (CBC) (plasma, K3 EDTA, Iowa State University College of Veterinary Medicine);
    - Standard chemistry panel, including alanine aminotransferase (ALT), alkaline phosphatase (ALP), albumin, total protein, triglycerides, total cholesterol, blood urea nitrogen (BUN), serum creatinine, serum bicarbonates, calcium, phosphorus, chloride, sodium and potassium (serum, plain tube, Iowa State University College of Veterinary Medicine);
    - Fasting blood glucose (serum, plain tube, Iowa State University College of Veterinary Medicine);
    - Glucagon (serum, plain tube, Cornell University College of Veterinary Medicine. *EMD Millipore's Glucagon Radioimmunoassay (RIA) Kit GL-32 K*);
    - Lipid profiling: HDL and Low-Density Lipoprotein (LDL) cholesterol (serum, plain tube, Texas A&M College of Veterinary Medicine);
    - Renin-angiotensin aldosterone system (RAAS) biomarkers (serum, plain tube, Attoquant Diagnostics, Vienna);
    - N-terminal prohormone of brain natriuretic peptide (NT-proBNP) (plasma, K3 EDTA, IDEXX Laboratories, Maine. *Cardiopet ProBNP Test-Canine*);
    - Oxidative stress biomarkers (serum, plain tube, University of Murcia Facultad de Veterinaria);
    - Metabolomics, including (1) General Metabolism; (2) Complex Lipids and (3) Biogenic Amines (serum, plain tube, University of California Davis Genome Center).

Composition
Dehydrated poultry protein, maize, rice, wheat, animal fats, maize gluten, hydrolyzed animal proteins, vegetable fibers, vegetable protein isolate, beet pulp, minerals, fish oil, yeasts, soya oil, psyllium husks and seeds, fructo-oligo-saccharides, hydrolyzed yeast (source of manno-oligo-saccharides), borage oil, green tea and grape extracts (source of polyphenols), hydrolyzed crustaceans (source of glucosamine), marigold extract (source of lutein), hydrolyzed cartilage (source of chondroitin) Nutritional additives: Vitamin A: 28,000 IU, Vitamin D3: 700 IU, E1 (Iron): 42 mg, E2 (Iodine): 4.2 mg, E4 (Copper): 5 mg, E5 (Manganese): 55 mg, E6 (Zinc): 164 mg, E8 (Selenium): 0.09 mg
Analytical constituents
Protein: 27% Fat content: 12% Crude ash: 6.1% Crude fibers: 3.7% EPA and DHA fatty acids: 3 g/kg

Table 1. Nutritional information of the Royal Canin® Beagle adult diet. Eighteen healthy adult Beagle dogs were fed a commercial diet (Royal Canin® Beagle Adult dry food) once in the morning, around 9 a.m. The portion size for each dog was calculated based on weight and resting energy requirements (RER). Information was provided on the food manufacturer's website (https://www.royalcanin.com/my/dogs/products/retail-products/beagle-adult-2106#). This diet contains 3463 kilocalories of metabolizable energy (ME) per kilogram or 284 kilocalories of ME per cup on an as-fed basis (calculated).

2A		
Parameter	**Target**	**Actual**
Energy (kcal)	1000.0	1000.3
Protein (g/Mcal)	40.1	40.3
Fat (g/Mcal)	40.8	40.9
CHO (g/Mcal)	118.3	117.9
Fiber (g/Mcal)	8.4	8.4
Sugar (g/Mcal)	51.4	51.4
Saturated fat (%)	37.0	36.4
Macronutrients		
% calories from Protein: 16.1%		
% calories from Fat: 36.8%		
% calories from CHO: 47.1%		
2B		
Ingredient	**g per 1000 kcal**	**Amount (g) for a typical 8.5 kg dog**
Proteins		
Ground beef, 80% lean	56.0	35.1
Egg protein powder	9.8	6.1
Carbohydrates		
Wheat bread	99.0	62.1
White bread	70.0	43.9
Light corn syrup	47.0	29.5
Fat		
Corn oil	11.0	6.9
Unsalted butter	15.5	9.7
Supplements		
Psyllium husk	3.0	1.9
Iodized salt	5.0	3.1
Balance.it® Canine K	14.4	9
Welactin Canine liquid	0.5 (mL)	0.3 (mL)

Table 2. Nutritional characteristics (2A) and composition (2B) of the western diet. Eighteen healthy adult Beagle dogs were fed a high-fat, high-monosaccharide, low-fiber Western diet (WD) adjusted from parameters of the National Health and Nutrition Examination Survey (NHANES) for a period of ten weeks. The dogs were provided with isocaloric feedings based on their individually calculated metabolizable energy. The diets were home cooked and offered to the dogs once daily in the morning, typically around 9 a.m.

- Serum insulin concentrations were measured on a separate day through an oral glucose tolerance test (plain tube, Michigan State University Veterinary Diagnostic Laboratory. *EMD Millipore's Insulin Radioimmunoassay (RIA) Kit HI-14K*). The dogs received an oral dose of 5 g of dextrose per kg in the form of a solution containing 1 g of dextrose powder per mL of water. Blood samples were collected at 30, 60, 90, 120, and 180 min after oral administration of the glucose solution.
- Voided urine and fecal samples were collected at ***BAS1*** and ***BAS2*** for the purpose of conducting metabolomic analyses, including (1) General Metabolism; (2) Complex Lipids and (3) Biogenic Amines (University of California Davis Genome Center).
- Serum, plasma, urine, and fecal samples were divided into separate aliquots and stored at − 80 °C prior to analysis.
- BP was measured at ***BAS1*** and ***BAS2*** by a certified cardiologist using a Doppler device, following standard procedures from the American College of Veterinary Internal Medicine (ACVIM), as outlined in consensus panel guidelines[48]. As Doppler-derived single measurements of blood pressure are an estimate of systolic blood pressure (SBP)[125], the abbreviation SBP will be used throughout this manuscript. To avoid any potential disruptions or bias in the recordings, these measurements were consistently taken before any blood was collected during each study period. To follow the consensus panel guidelines for assessing hypertension[48] and ensure accuracy, five consecutive and consistent SBP measurements were obtained from each subject. These values were then averaged to calculate an individual estimate of SBP.

Specific analytical methods

Lipoprotein profiling

Lipoprotein profiling was carried out using the continuous lipoprotein density profiling (CLPDP) method, adhering to procedures detailed in prior literature[49,50]. Briefly, a solution of 0.18 M NaBiEDTA (Tokyo Chemical

Industry) measuring 1280 µL was combined with 10 µL of both serum and NBD C6-ceramide (Cayman Chemical Company). Subsequently, 1150 µL of the resultant blend was allocated to a polycarbonate centrifuge container (Beckman Coulter). The samples underwent centrifugation for 6 h at 4 °C and 867,747 g using an Optima MAX-LP ultracentrifuge (Beckman Coulter) equipped with a fixed-angle rotor (MLA-130; Beckman Coulter). Immediately post-centrifugation, the samples were imaged using a fluorescence imaging system comprising a digital camera (Quantifire XI; Optronics) and a constant metal halide light source (Dolan-Jenner Industries).

The images obtained were transformed into density profiles via software analysis (OriginPro7.5; OriginLab). Lipoprotein profiles were produced by plotting the average intensity of fluorescence on the y-axis, while the actual centrifuge tube coordinates (mm) served as the x-axis. A unique numbering system was established for the statistical examination. The area under the curve (AUC) of the total fluorescence trace and each segment were used to determine the total lipoprotein intensity and fractional intensities, respectively. AUCs were then calculated for LDLs and HDLs based on their density intervals. Individual AUC values were finally normalized using the total AUC and expressed as percentage, as presented by Minamoto et al.[50].

RAAS fingerprinting

Determination of angiotensin and aldosterone analytes from canine serum was derived as previously published by our consortium[51–54]. Briefly, serum samples were analyzed to determine the equilibrium concentrations of Angiotensin I (Ang I (1–10)), Angiotensin II (Ang II (1–8)), Angiotensin III (Ang III (2–8)), Angiotensin IV (Ang IV (3–8)), Angiotensin 1–7 (Ang1–7), Angiotensin 1–5 (Ang1–5), and aldosterone using validated Liquid Chromatography-Tandem Mass Spectrometry (LC–MS/MS) assays at a commercial laboratory (Attoquant Diagnostics, Vienna, Austria)[55]. Following ex vivo equilibration, each sample was spiked with a stable isotope-labeled internal standard for each angiotensin peptide and a deuterated internal standard for aldosterone (aldosterone D4). The analytes were then extracted using C18-based solid-phase extraction. The extracted samples underwent mass spectrometry analysis using a reversed-analytical column, which was operated in tandem with a XEVO TQ-S triple quadrupole mass spectrometer in multiple reaction monitoring mode. Internal standards were used to ensure analyte recovery throughout the sample preparation process for each sample. The concentrations of the analytes were calculated from the chromatograms where the integrated signals exceeded a signal-to-noise ratio of 10, considering the corresponding response factors derived from appropriate calibration curves in the serum matrix. The lower limit of quantification (LLOQ) was established at 3.0 pM, 2.0 pM, 3.0 pM, 2.0 pM, 2.5 pM, 2.0 pM and 13.9 pM for Ang I (1–10)), Ang II (1–8), Ang1–7, Ang1–5, Ang III (2–8), Ang IV (3–8) and aldosterone, respectively. Markers for renin (PRA–S) and angiotensin-converting enzyme (ACE–S) based on angiotensin were obtained from Ang II (1–8) and Ang I (1–10) concentrations by calculating their sum and ratio, respectively[56]. Renin-independent alternative RAAS activation (ALT–S) was calculated using the formula [(Ang 1–7 + Ang 1–5) / (Ang I + Ang II + Ang 1–7 + Ang 1–5)][57].

Oxidative stress markers

The development and validation of analytical techniques for assessing oxidative stress markers adhered to protocols outlined in previous studies[58]. The following provides an abridged overview of the specific procedures used in evaluating antioxidant and oxidant statuses.

Antioxidant status.

- The *Cupric Reducing Antioxidant Capacity* (**CUPRAC**) assay, initially described by Campos et al.[59], is based on the conversion of Cu^{2+} to Cu^{+} through the action of non-enzymatic antioxidants in the serum sample. Quantification of CUPRAC followed the protocol previously validated for canine serum[60], with results reported in mmol/L.
- The *Ferric Reducing Ability of Plasma* (**FRAP**) assay relies on the conversion of ferric-tripyridyltriazine (Fe^{3+}-TPTZ) to its ferrous form[61]. Quantification of FRAP was performed as described in previous studies[60,61]. Results are expressed in mmol/L.
- Measurements of *Trolox Equivalent Antioxidant Capacity* (**TEAC**) followed the procedures outlined by Arnao et al.[62] later adapted to canine serum samples by Rubio et al.[60]. The assay involves the generation of ABTS radicals and their subsequent reduction by non-enzymatic antioxidants in the serum specimen[62], with results presented in mmol/L.
- **Total thiol** (µmol/L) determination was based on the reaction between sample thiols and DTNB[126,63].
- The evaluation of *Paraoxonase type 1* (**PON-1**) was based on the conversion of phenylacetate to phenol, following the same methods used for canine serum by Tvarijonaviciute et al.[64]. Results are expressed as IU/mL.
- Quantification of *Glutathione Peroxidase* (**GPx**) activity was performed using a commercial assay kit according to the manufacturer's instructions (*RANDOX Glutathione Peroxidase (Ransel) Kit RS504*), as described in previous studies[65,66]. Results are reported in IU/ml units.

Oxidant status.

- The *Total Oxidant Status* (**TOS**) was determined following Erel's method[67], which had previously been applied to dog serum[60]. Results are expressed in µmol/L.

- The *Peroxide-Activity* (**POX-Act**) assay involved the detection of total peroxides through a peroxide-peroxidase reaction using tetramethylbenzidine as the chromogenic substrate[68]. Results are expressed in µmol/L.
- The *Derivatives-Reactive Oxygen Metabolites* (**d-ROMs**) assay used an acidic medium to react with the sample in the presence of DEPPD, as per the method previously established by Alberti et al.[69]. Results are reported in Carratelli Units (U.CARR).
- Determination of *Advanced Oxidation Protein Products* (**AOPP**) was based on oxidized albumin and di-tyrosine containing cross-linked proteins, as described in previous studies[70,71]. Results are expressed in µmol/L.

Serum/urine/fecal metabolomics

General metabolism. Samples were extracted using the extraction procedure by Matyash et al.[72], which includes MTBE, MeOH, and H_2O. The organic (upper) phase was dried down and submitted for resuspension and injection onto the LC, while the aqueous (bottom) phase was dried down and submitted for derivatization for GC. Samples were shaken at 30 °C for 1.5 h. Then, 91 µL of MSTFA + FAMEs were added to each sample, and tubes were shaken at 37 °C for 0.5 h to complete the derivatization. Samples were then vialed, capped, and injected onto the instrument. A 7890A GC coupled with a LECO time of flight mass spectrometer (TOFMS) was used for the procedure. Then, 0.5 µL of the derivatized sample was injected using a splitless method onto a RESTEK RTX-5SIL MS column with an Intergra-Guard at 275 °C with a helium flow of 1 mL/min. The GC oven was set to hold at 50 °C for 1 min, then ramped up to 20 °C/min to 330 °C and held for 5 min. The transfer line was set to 280 °C, while the EI ion source was set to 250 °C. The mass spectrometry parameters collected data from 85 to 500 m/z at an acquisition rate of 17 spectra/second. All compounds detected were tentatively identified to the Metabolomics Standards Initiative (MSI) Level 2 with a spectral library match score of 800 or higher[73].

Complex lipids. Samples were extracted using the extraction procedure by Matyash et al.[72], which includes MTBE, MeOH, and H_2O. The organic (upper) phase was dried down and resuspended for injection onto the LC, while the aqueous (bottom) phase was dried down and submitted for derivatization for GC. The samples were then resuspended with 110 µL of a solution of 9:1 methanol:toluene and 50 ng/mL CUDA. Samples were then shaken for 20 s, sonicated for 5 min at room temperature, and centrifuged for 2 min at 16100 rcf. Thirty-three µL of samples were aliquoted into a vial with a 50 µL glass insert for positive and negative mode lipidomics. The samples were then loaded onto an Agilent 1290 Infinity LC stack. The positive mode was run on an Agilent 6546 with a scan range of m/z 120–1200 Da and an acquisition speed of 2 spectra/s. Positive mode had between 0.5 and 2 µL injected onto an Acquity Premier BEH C18 1.7 µm, 2.1 × 50 mm column. The gradient used was 0 min 15% (B), 0.75 min 30% (B), 0.98 min 48% (B), 4.00 min 82% (B), 4.13–4.50 min 99% (B), 4.58–5.50 min 15% (B) with a flow rate of 0.8 mL/min. Another aliquot was run in negative mode on an Agilent 1290 Infinity LC stack and injected onto the same column, with the same gradient, using an Agilent 6550 QTOF mass spectrometer. The acquisition rate was two spectra per second with a scan range of m/z 60–1200 Da. The mass resolution for the Agilent 6530 is 10,000 for ESI (+) and 20,000 for ESI (-) for the Agilent 6550.

Biogenic amines. Sample extraction for biogenic amines consisted of a liquid–liquid extraction method[72] with MTBE, methanol, and water, creating a biphasic partition. The polar phase was then dried down to completion and run on a Waters Premier Acquity BEH Amide column. A short 4-min liquid chromatography method was used for the separation of polar metabolites from a starting condition of 100% LCMS H_2O with 10 mM ammonium formate and 0.125% formic acid to an end condition of 100% ACN:H_2O 95:5 (v/v) with 10 mM ammonium formate and 0.125% formic acid. A Sciex Triple-ToF scanned from 50 to 1500 m/z with MS/MS collection from 40 to 1000, selecting the top five ions per cycle. Data processing was done with MS-Dial using an MZ-RT list for annotations, in addition to a library for MS/MS matching.

Statistics

The sample size for this experiment was established based on preliminary data from a previous study conducted by our group[44]. In that study, statistically significant differences in BP and total cholesterol were observed in a group of ten dogs receiving an isocaloric WD, with an alpha level of 0.05 and a statistical power of 80%. Study variables were visually inspected for normality, summarized, and displayed as median (interquartile range [IQR]). The area under the curve for insulin time-concentrations in the serum was determined by using the linear trapezoidal method from 0 to 90 min ($AUC_{ins(0-90)}$). Differences between ***BAS1*** and ***BAS2*** were analyzed using non-parametric Wilcoxon signed rank test with continuity correction. *P*-values < 0.05 were considered statistically significant. The R software version 4.2.2 was used for statistical analyses. (R Core Team (2022). Graphical representation of the data was produced using the *ggplot2* package in R version 4.2.2. For metabolomic analyses, the peak tables were uploaded into the Matlab® (R2023b, The Mathworks Inc., Natick, MA) environment and converted to datasets with appropriate class labels. In PLS_Toolbox (Version 9.0; Eigenvector Research, Manson, WA), a Principal Component Analysis (PCA) was performed on the autoscaled data. To determine the variables responsible for differences between groups, a Cluster Resolution Feature Selection (FS-CR) was applied[74,75]. For each dataset, the FS-CR process of sequential backward elimination and forward selection was repeated 100 times, permuting the subsets of data, and only variables selected 85% of the time were retained to prevent overfitting[75]. The distance between clusters (cluster resolution) was used to determine which variables contributed to the separation between classes[75]. A PCA was then performed using the selected variables from the FS-CR, and the variables and their loadings were extracted. PCA score plots were generated to visualize the

relationships between samples and classes, with a 95% confidence interval plotted around the mean center of the data.

Results

Physical examination and adverse events

The study veterinarian, along with approved study personnel, conducted weekly physical examinations and reported no notable changes in the dogs' overall condition, behavior, cardiovascular system, hydration level, respiratory system, or skin appearance throughout the study.

During the transition from their regular diet (Royal Canin® Beagle Adult) in the first baseline phase (***BAS1***) to the Western diet (***BAS2***), several dogs experienced one or more episodes of softened stools. These instances were considered "on-serious" digestive adverse events by the study veterinarian and resolved on their own within a few days. No significant adverse effects were reported over the duration of the study.

Body weight

Differences in body weight between diets (− 3.6% based on median relative change from ***BAS1***) were statistically significant but were not considered clinically meaningful by the study veterinarian (***BAS1*** 8.9 [7.8–9.6] kg) vs. ***BAS2*** 8.7 [7.4–9.2] kg). Similarly, no notable changes in body condition scores were reported between ***BAS1*** (N = 0, 13 and 5 for "underweight", "ideal" and "overweight", respectively) and ***BAS2*** (N = 1, 11 and 6 for "underweight", "ideal" and "overweight", respectively).

Complete blood count and chemistry

All hematological parameters were within normal physiological limits, and there were no clinically relevant changes in CBC between ***BAS1*** and ***BAS2***.

No significant changes in liver-related chemical parameters, including ALT, ALP, albumin, and total protein, were observed between ***BAS1*** and ***BAS2***. However, dogs fed a WD for ten weeks had a decrease in serum bicarbonate (− 2.5 [− 4.0 to − 1.0] mEq/L, $P < 0.001$), phosphorus (− 0.8 [− 1.3 to − 0.5] mg/dL, $P < 0.001$), and potassium (− 0.5 [− 0.7 to − 0.3] mEq/L, $P < 0.001$), and an increase in chloride concentrations (+ 1.5 [0.0–3.0] mEq/L, $P = 0.001$). The diet also induced some borderline statistically significant changes in calcium ($P = 0.049$) and sodium ($P = 0.041$) levels at ***BAS2***. Additionally, there was a significant decrease in BUN at ***BAS2*** (− 4.5 [− 5.0 to − 3.0] mg/dL, $P < 0.001$), along with an increase in serum creatinine (+ 0.1 [0.0–0.2] mg/dL, $P = 0.001$). These variations, although statistically significant, remained within physiological limits. A summary of the clinical chemistry parameters at ***BAS1*** and ***BAS2*** is presented in Fig. 2.

Fasting blood glucose, serum glucagon and insulin

The biological effects of the WD on fasting blood glucose, as well as the glucose-regulating hormones glucagon and insulin, are presented in Figs. 3 and 4. Over a span of ten weeks, the WD induced a significant increase in fasting blood glucose concentrations (Fig. 3). This increase approached the upper physiological limit, demonstrating an overall increase of 15.8% relative to baseline (***BAS1*** 88.0 [82.0–91.0] mg/dL vs. ***BAS2*** 102.5 [95.0–109.0] mg/dL, $P < 0.001$). The increase in fasting blood glucose was accompanied by a non-significant trend suggesting a decrease in serum glucagon levels at ***BAS2*** (***BAS1*** 69.3 [64.0–77.2] pg/mL vs. ***BAS2*** 61.8 [49.8–64.3] pg/mL, $P = 0.055$).

Additionally, the results of the glucose tolerance test suggest a trend towards an elevation in peak insulin concentrations in dogs fed a WD. The median $AUC_{ins(0-90)}$ showed a 34.9% increase from 202.7 [103.1–276.8] uIU/mL x min at ***BAS1*** to 232.7 [144.2–276.2] uIU/mL x min at ***BAS2*** ($P = 0.39$). The average (arithmetic mean) for this increase at ***BAS2*** was 58.2% (Fig. 4).

Blood pressure

Overall, SBP measurements were significantly higher at ***BAS2*** compared with pre-WD readings (***BAS1*** 133.5 [126.0–141.0] mmHg vs. ***BAS2*** 143.0 [133.0–152.0] mmHg, $P = 0.017$) (Fig. 5A).

NT-proBNP

NT-proBNP levels significantly increased at ***BAS2***, as shown by the change from baseline (***BAS1*** 250.0 [250.0–401.0] pmol/L) to post-WD (***BAS2*** 460.5 [330.0–750.0] pmol/L) ($P < 0.001$) (Fig. 5B). Notably, two dogs exhibited NT-proBNP concentrations exceeding 900 pmol/L.

Renin-angiotensin aldosterone system (RAAS)

Our analysis revealed a slight downward trend in biomarkers in both the traditional and alternative arms of the RAAS, though this trend was not statistically significant. This included reductions in plasma renin activity (PRA–S), Angiotensin I (Ang I (1–10)), Angiotensin II (Ang II (1–8)), Angiotensin III (Ang III (2–8)), Angiotensin IV (Ang IV (3–8)), Angiotensin 1–7 (Ang1–7), and Angiotensin 1–5 (Ang1–5). Aldosterone data was not available for statistical analysis, as over 45% of the samples had analyte levels below the lower limit of quantification. A comprehensive overview of the RAAS biomarker profile is provided in Table 3.

Total cholesterol, triglycerides and lipoproteins

Figure 6 summarizes the impact of the WD on total cholesterol, HDL-cholesterol, and LDL-cholesterol. After ten weeks of feeding with the WD, there was a 44.0% increase in total cholesterol concentrations (from ***BAS1*** 130.0 [125.0–145.0] mg/dL to ***BAS2*** 187.5 [173.0–219.0] mg/dL, $P < 0.001$), along with a significant reduction in

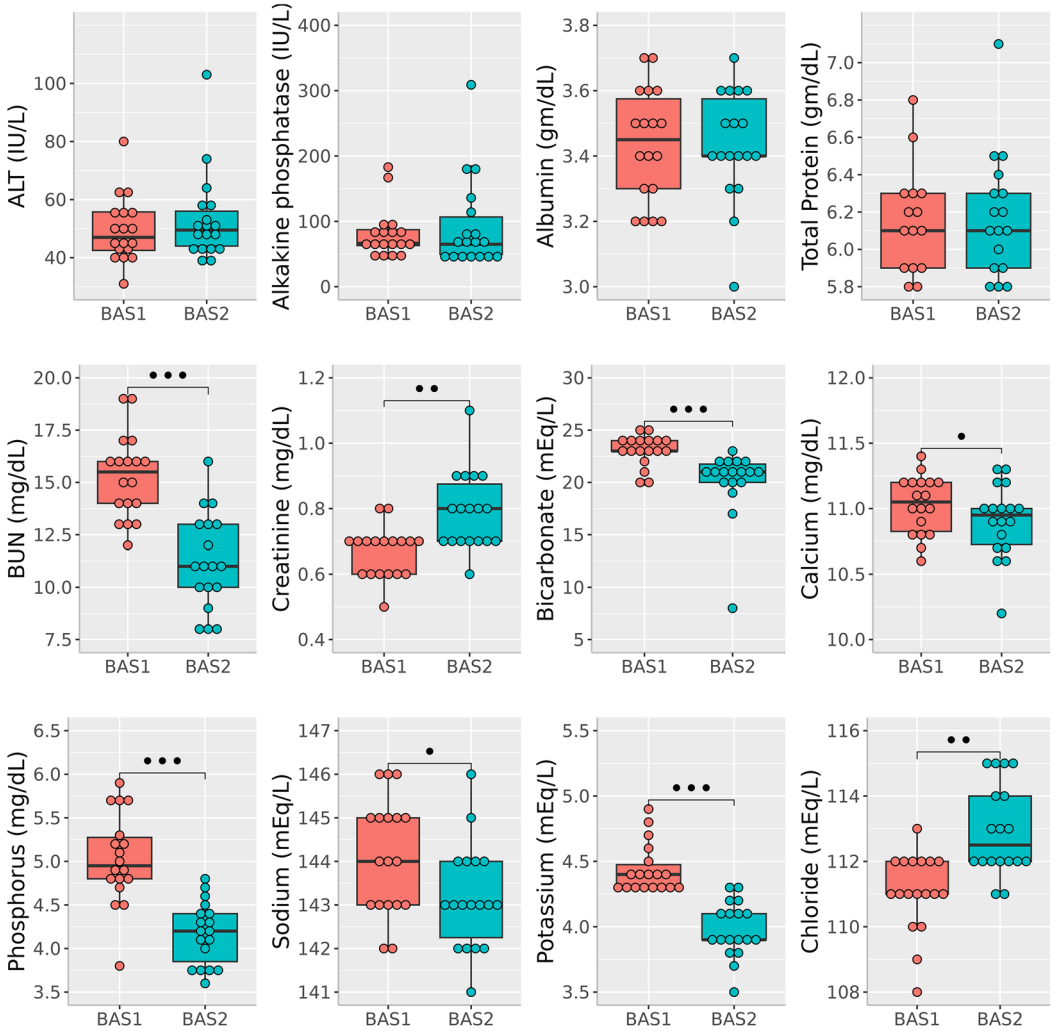

Fig. 2. Temporal changes in standard clinical chemistry parameters after ten weeks of feeding with a high-fat, high-monosaccharide, low-fiber western diet. No notable alterations were observed in liver-related chemical parameters, such as ALT, ALP, albumin, and total protein, when comparing ***BAS1*** to ***BAS2***. Dogs at ***BAS2*** had decreased levels of serum bicarbonates, phosphorus, and potassium, but increased levels of chloride. There was also a reduction in BUN at ***BAS2***, along with an elevation in serum creatinine levels. Box plots represent the 25th, 50th and 75th percentile of the data ± 1.5 IQR (interquartile range). •: $0.01 < P \leq 0.05$; ••: $0.001 < P \leq 0.01$; •••: $P \leq 0.001$. Summary box plots produced using the *ggplot2* package in R version 4.2.2.

the AUC percentage of HDL-cholesterol (from ***BAS1*** 84.2 [80.0–85.6] % to ***BAS2*** 81.1 [73.8–83.1] %, $P < 0.001$) and a 26.8% elevation in the AUC percentage of LDL-cholesterol (from ***BAS1*** 14.5 [13.0–17.0] % to ***BAS2*** 18.0 [15.5–24.5] %, $P < 0.001$). Looking at the distribution of the *absolute* values for each lipoprotein fraction, the absolute HDL-cholesterol concentrations increased from ***BAS1*** (6,977.7 [6,091.7–7,319.3] fluorescence intensity (FI)) to ***BAS2*** (8,029.1 [6,998.5–8,346.4] FI) ($P = 0.008$). However, this increase was more pronounced for the absolute LDL-cholesterol concentrations (***BAS1*** 1,206.5 [976.8–1,505.8] FI vs. ***BAS2*** 1,857.2 [1,293.9–2,467.8] FI, $P < 0.001$), suggesting that the WD increased total cholesterol and caused a shift from HDL-cholesterol to LDL-cholesterol. The detailed lipoprotein profiles, including levels at both baseline (***BAS1)*** and post-WD feeding (***BAS2***), along with their statistical significance, are presented in Table 4. Overall, besides the changes in the AUC percentages of total HDL and total LDL-cholesterol, the WD caused a significant decrease in HDL 2a ($P < 0.001$), which are larger and less dense subfractions of HDL-cholesterol. Additionally, the WD induced a significant increase in LDL 3 and LDL 4 ($P < 0.001$), which are small and dense subfractions of LDL-cholesterol. Notably, these changes were not accompanied by significant alterations in serum triglyceride concentrations (***BAS1*** 38.0 [33.0–45.0] mg/dL vs. ***BAS2*** 37.5 [34.0–48.0] mg/dL, $P = 0.54$).

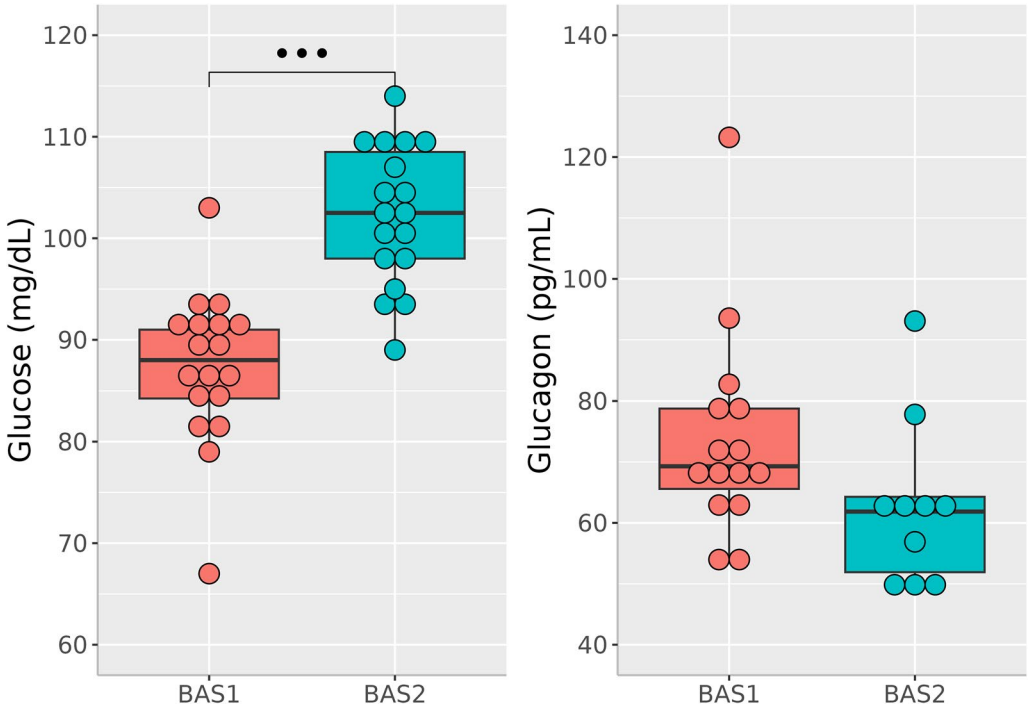

Fig. 3. Temporal changes in fasting blood glucose and glucagon after ten weeks of feeding with a high-fat, high-monosaccharide, low-fiber western diet. The WD resulted in a significant 16.5% increase in fasting blood glucose, approaching the upper physiological limit. This was accompanied by a trend towards lower serum glucagon levels which did not reach statistical significance. Box plots represent the 25th, 50th and 75th percentile of the data ± 1.5 IQR (interquartile range). •••: $P \leq 0.001$. Summary box plots produced using the *ggplot2* package in R version 4.2.2.

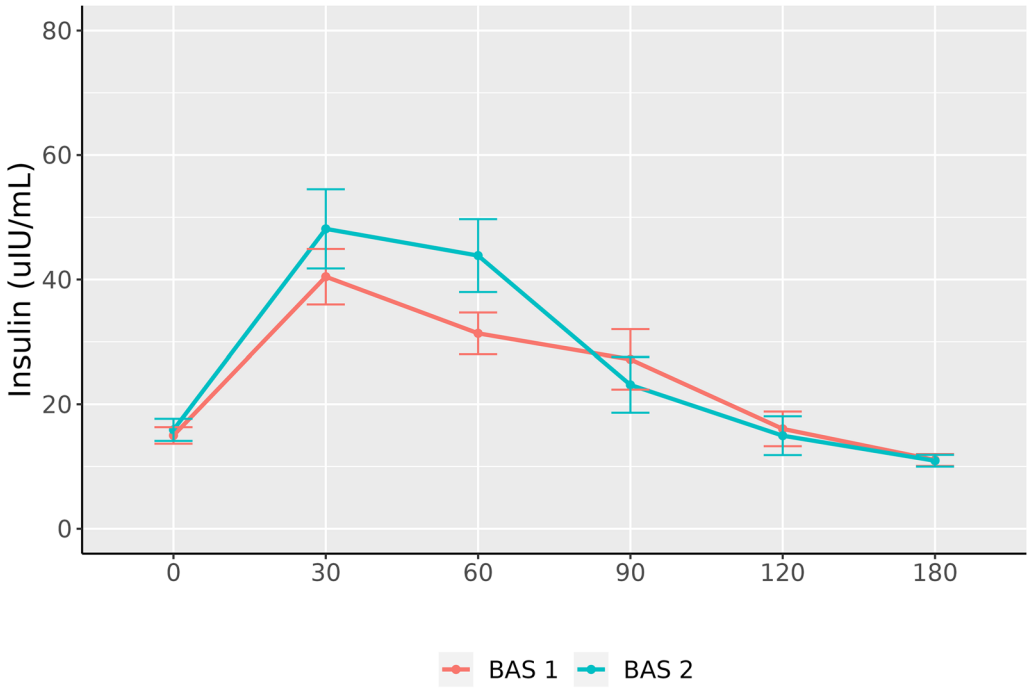

Fig. 4. Serum insulin time-course post-glucose tolerance test. Dogs received an oral dose of 5 g of dextrose per kg in the form of a solution containing 1 g of dextrose powder per mL of water. Blood samples were collected at 30, 60, 90, 120, and 180 min after oral administration of the glucose solution. Compared to ***BAS1***, dogs fed an isocaloric WD for ten weeks showed a trend towards a higher peak concentration of insulin, with an increase of approximately 35% in $AUC_{ins(0-90)}$ at ***BAS2***. Time-course data are presented as mean ± S.E. Scatter plots produced using the *ggplot2* package in R version 4.2.2.

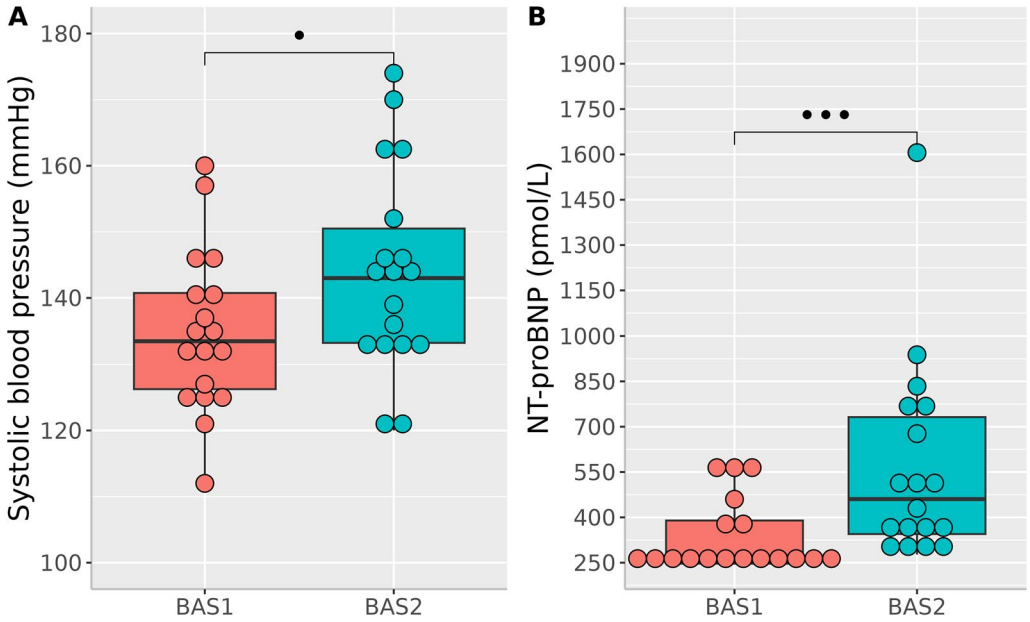

Fig. 5. Temporal changes in systolic blood pressure (**A**) and NT-proBNP (**B**) after ten weeks of feeding with a high-fat, high-monosaccharide, low-fiber western diet. (**A**) Dogs fed a WD for ten weeks had significantly higher blood pressure measurements compared with baseline (***BAS1***). Measures were taken by a certified cardiologist using a Doppler device. To avoid bias in the recordings, these measurements were consistently taken before any blood was collected during each study period. To follow the ACVIM consensus panel guidelines for assessing hypertension[48] and ensure accuracy, five consecutive and consistent SBP measurements were obtained from each subject. These values were then averaged to calculate an individual estimate of SBP. (**B**) NT-proBNP concentrations significantly increased at ***BAS2***, with two dogs presenting values exceeding 900 pmol/L, a level commonly associated with structural heart disease in canines[94,95]. Box plots represent the 25th, 50th and 75th percentile of the data ± 1.5 IQR (interquartile range). •: $0.01 < P \leq 0.05$; •••: $P \leq 0.001$. Summary box plots produced using the *ggplot2* package in R version 4.2.2.

Variable	BAS1	BAS2	*P*-value
Ang I (1–10)	100.7 (70.7–114.5)	71.6 (40.3–102.3)	0.30
Ang II (1–8)	68.8 (40.8–81.3)	45.4 (25.4–91.7)	0.62
Ang III (2–8)	14.8 (8.4–15.4)	11.0 (7.7–12.3)	0.68
Ang IV (3–8)	13.7 (10.3–15.8)	7.6 (5.5–11.6)	0.11
Ang (1–7)	25.5 (11.7–35.2)	17.1 (9.0–19.0)	0.42
Ang (1–5)	57.9 (34.7–70.6)	35.4 (25.1–54.2)	0.30
ACE–S	0.68 (0.57–0.72)	0.64 (0.52–0.68)	0.73
PRA–S	176.8 (121.8–194.5)	106.9 (67.5–196.5)	0.42
ALT–S	0.34 (0.28–0.38)	0.32 (0.27–0.39)	0.62

Table 3. Effect of the western diet model on biomarkers of the Renin-angiotensin aldosterone system (RAAS). Pharmacodynamic changes in both the classical and alternative arm of the RAAS after ten weeks of feeding with a high-fat, high-monosaccharide, low-fiber Western diet (WD), including: Angiotensin I (Ang I (1–10)), Angiotensin II (Ang II (1–8)), Angiotensin III (Ang III (2–8)), Angiotensin IV (Ang IV (3–8)), Angiotensin 1–7 (Ang1–7), and Angiotensin 1–5 (Ang1–5). Markers for renin (PRA–S) and angiotensin-converting enzyme (ACE–S) based on angiotensin were obtained from Ang II (1–8) and Ang I (1–10) levels by calculating their sum and ratio, respectively[56]. Renin-independent alternative RAAS activation (ALT–S) was calculated using the formula [(Ang 1–7 + Ang 1–5) / (Ang I + Ang II + Ang 1–7 + Ang 1–5)], as previously described[57].

Oxidative stress

Antioxidant status

Overall, the effect of the WD on antioxidant markers was mild, with no significant changes in CUPRAC, FRAP, TEAC, and Thiol values. In contrast, PON-1 levels significantly decreased at ***BAS2*** compared to ***BAS1*** (***BAS1*** 4.2 [3.7 to 4.4] IU/mL vs. ***BAS2*** 3.8 [3.6–4.0] IU/mL, $P = 0.004$), and GPx activity increased significantly at ***BAS2*** (***BAS1*** 6460.0 [5448.0–7764.0] U/L vs. ***BAS2*** 8,432.0 [6964.0–8852.0] U/L, $P < 0.001$). These effects are summarized in Fig. 7A.

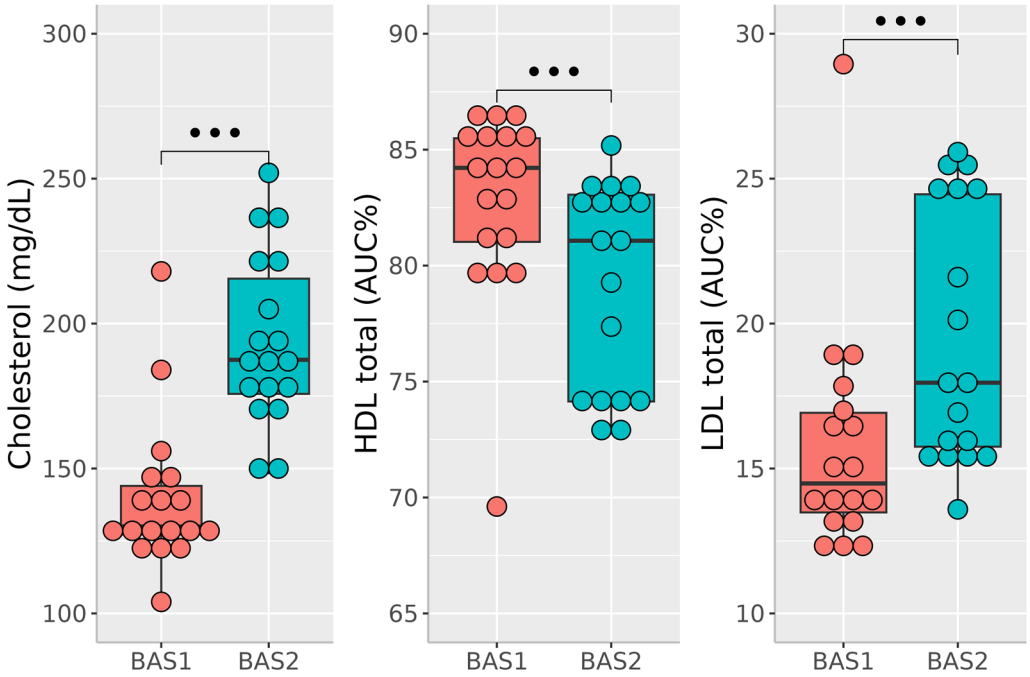

Fig. 6. Temporal changes in total cholesterol, HLD-cholesterol and LDL-cholesterol after ten weeks of feeding with a high-fat, high-monosaccharide, low-fiber western diet. Circulating levels of cholesterol were significantly increased (+44.2%) after ten weeks of feeding with the isocaloric WD. Notably, this change was accompanied by a significant reduction in HDL-cholesterol and a 26.8% elevation in LDL-cholesterol. Box plots represent the 25th, 50th and 75th percentile of the data ± 1.5 IQR (interquartile range). •••: $P \leq 0.001$. Summary box plots produced using the *ggplot2* package in R version 4.2.2.

Variable	BAS1	BAS2	*P*-value
HDL 2a (AUC%)	28.3 (26.4–28.8)	24.7 (21.8–27.1)	< 0.001
HDL 2b (AUC%)	21.4 (18.4–23.3)	21.1 (19.2–22.2)	0.39
HDL 3a (AUC%)	25.1 (23.2–27.9)	24.6 (22.4–26.2)	0.14
HDL 3b (AUC%)	7.1 (6.0–8.0)	7.4 (6.5–8.7)	0.13
HDL 3c (AUC%)	1.2 (1.0–1.3)	1.3 (1.0–1.5)	0.61
HDL total (AUC%)	**84.2 (80.0–85.6)**	**81.1 (73.8–83.1)**	**< 0.001**
LDL 1 (AUC%)	0.6 (0.5–0.8)	0.6 (0.5–0.7)	0.44
LDL 2 (AUC%)	1.4 (1.2–1.5)	1.5 (1.2–1.7)	0.30
LDL 3 (AUC%)	2.6 (2.4–3.5)	4.8 (3.9–6.9)	< 0.001
LDL 4 (AUC%)	4.1 (3.7–4.9)	5.2 (4.4–6.8)	< 0.001
LDL 5 (AUC%)	6.1 (4.9–6.7)	6.2 (5.0–7.4)	0.26
LDL total (AUC%)	**14.5 (13.0–17.0)**	**18.0 (15.5–24.5)**	**< 0.001**

Table 4. Effect of the western diet model on circulating lipoprotein fractions. Total values for HDL and LDL are indicated in bold. Lipoprotein profiles were produced by plotting the average intensity of fluorescence on the y-axis, while the actual centrifuge tube coordinates (mm) served as the x-axis. A unique numbering system was established for statistical examination. The area under the curve (AUC) of the total fluorescence trace and each segment were used to determine the total lipoprotein intensity and fractional intensities, respectively. Moreover, AUCs were calculated for high-density lipoproteins (HDLs) and low-density lipoproteins (LDLs), based on their density intervals. These AUC values were normalized using the total AUC and expressed as percentage, as previously presented by Minamoto et al.[50].

Oxidant status

The impact of the WD on oxidative stress parameters was more consistent, with total oxidant status significantly increasing at ***BAS2*** (***BAS1*** 4.8 [3.9–5.8] µmol/L vs. ***BAS2*** 7.0 [4.9–8.7] µmol/L, $P = 0.018$). This also extended to an increase (trend) in reactive oxygen metabolites (***BAS1*** 21.3 [13.2–28.9] U.CARR vs. ***BAS2*** 28.8 [17.9–43.0] U.CARR, $P = 0.084$). Conversely, there was a decrease in POX-Act post-WD (***BAS1*** 101.8 [79.1–114.0] µmol/L vs. ***BAS2*** 92.3 [62.1–94.2] µmol/L, $P < 0.001$). However, there were no discernible effects on AOPP (Fig. 7B).

Metabolomics

For all three –omics evaluated (General Metabolism, Complex Lipids, and Biogenic Amines), significant differences were observed in the metabolomes between ***BAS1*** and ***BAS2***.

General metabolism

Before feature selection, a clear separation between ***BAS1*** and ***BAS2*** was observed in the PCAs for urine, stool, and serum (Fig. 8A–C). To identify variables responsible for this separation, FS-CR was further employed[74,75]. FS-CR identified 48 significant metabolites in the urine samples, 37 significant metabolites in stool samples, and 10 in serum samples. The loadings of the selected variables are included in the Supplementary Information (Supplementary Figs. S1–S3, S2–S6 and S7–S9, for *General Metabolism*, *Complex Lipids* and *Biogenic Amines*, respectively). Following feature selection, ***BAS1*** and ***BAS2*** were clearly separated along PC1 for all three sample types, which explained 29.4%, 48.6%, and 82.3% of the total variance for urine, stool, and serum samples, respectively (Fig. 9A–C).

In urine, 29 metabolites were positively correlated with ***BAS1***, including pipecolinic acid, piperidone, cytosine, and nicotinamide (Supplementary Table 1). Additionally, 19 metabolites were strongly positively correlated with ***BAS2***, including 2,3-dihydroxybutanoic acid (tartaric acid), arabitol, cellobiose, and glycerol (Supplementary Table 1).

In stool, seven metabolites were positively correlated with ***BAS1***, such as cadaverine, trans-4-hydroxyproline, tryptamine, and isopalmitic acid (Supplementary Table 2). Thirty metabolites were strongly positively correlated to ***BAS2***, including fructose, pipecolinic acid, erythrose, and 2-deoxyerythritol (Supplementary Table 2).

In serum, nine of the ten significant metabolites from FS-CR were positively correlated to ***BAS1***, including 3-Amino-2-piperidone and 2-picolinic acid (Supplementary Table 3).

In summary, the clear separation of ***BAS1*** and ***BAS2*** in PCA space before feature selection suggests that the WD is causing significant, measurable changes in the general metabolism of the dogs.

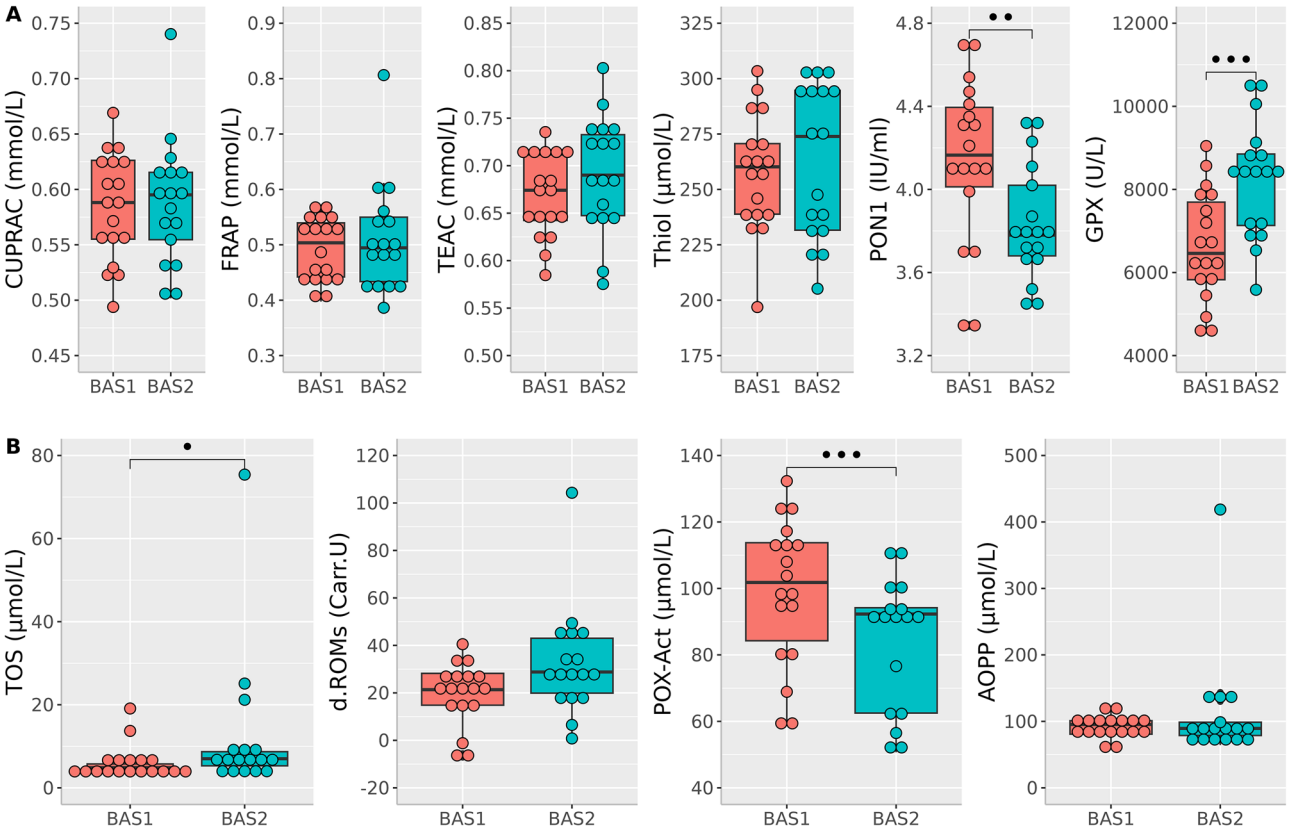

Fig. 7. Temporal changes in antioxidant (**A**) and oxidant (**B**) stress markers after ten weeks of feeding with a high-fat, high-monosaccharide, low-fiber western diet. The WD had mild effects on antioxidant markers, with no significant changes in CUPRAC, FRAP, TEAC, and Thiol values. However, PON-1 levels significantly decreased at ***BAS2***. The impact of the WD on oxidative stress parameters was more consistent, with total oxidant status significantly increasing at ***BAS2***. The increase extended to reactive oxygen metabolites (d-ROMs). Conversely, there was a decrease in POX-Act post-WD, but no notable effects on AOPP. Box plots represent the 25th, 50th and 75th percentile of the data ± 1.5 IQR (interquartile range). •: $0.01 < P \leq 0.05$; ••: $0.001 < P \leq 0.01$; •••: $P \leq 0.001$. Summary box plots produced using the *ggplot2* package in R version 4.2.2.

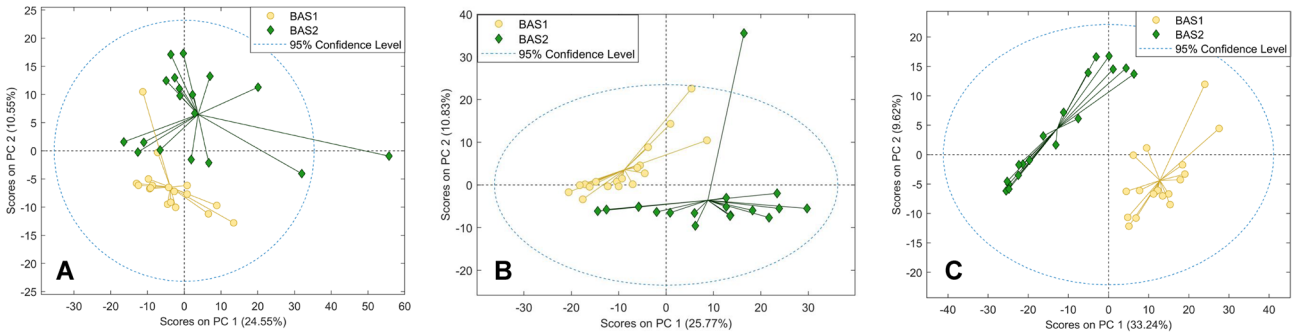

Fig. 8. PCA score plots (*General Metabolism*) of (**A**) Urine, (**B**) Stool, and (**C**) Serum *before* feature selection using the PLS_Toolbox software (Version 9.0; Eigenvector Research, Manson, WA).

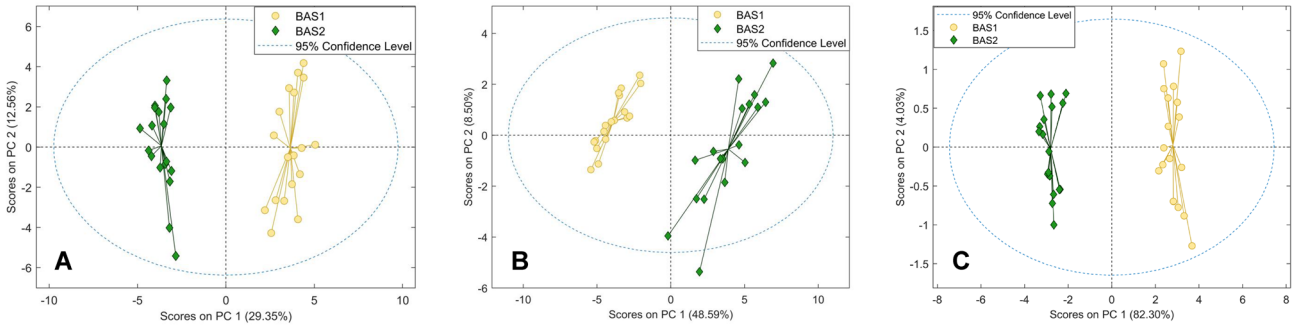

Fig. 9. PCA score plots (*General Metabolism*) of (**A**) Urine, (**B**) Stool, and (**C**) Serum *after* feature selection using the PLS_Toolbox software (Version 9.0; Eigenvector Research, Manson, WA).

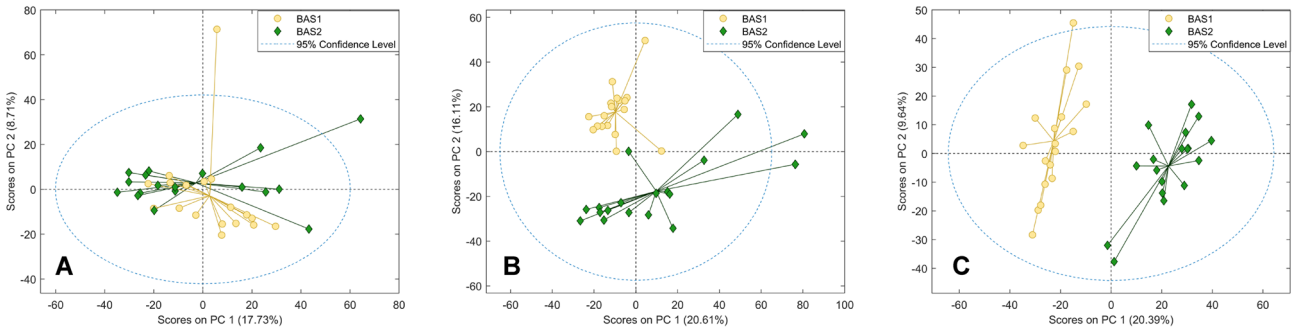

Fig. 10. PCA score plots (*Complex Lipids*) of (**A**) Urine, (**B**) Stool, and (**C**) Serum *before* feature selection using the PLS_Toolbox software (Version 9.0; Eigenvector Research, Manson, WA).

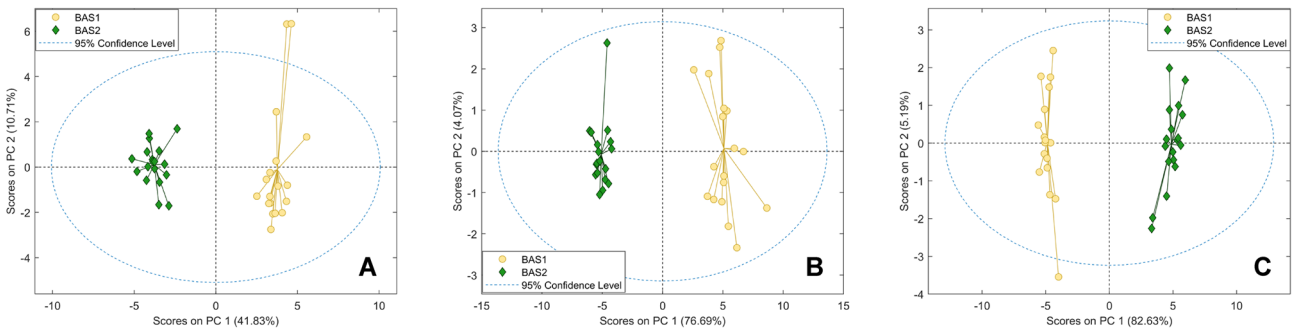

Fig. 11. PCA score plots (*Complex Lipids*) of (**A**) Urine, (**B**) Stool, and (**C**) Serum *after* feature selection using the PLS_Toolbox software (Version 9.0; Eigenvector Research, Manson, WA).

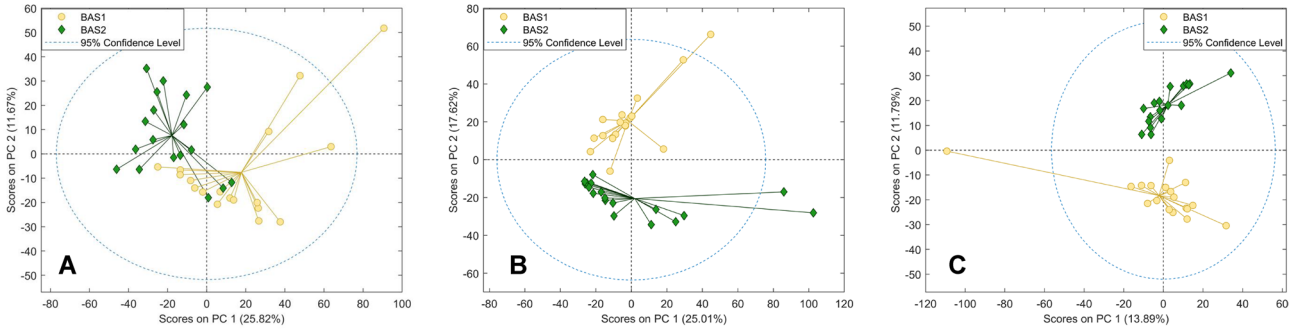

Fig. 12. PCA score plots (*Biogenic Amines*) of (**A**) Urine, (**B**) Stool, and (**C**) Serum *before* feature selection using the PLS_Toolbox software (Version 9.0; Eigenvector Research, Manson, WA).

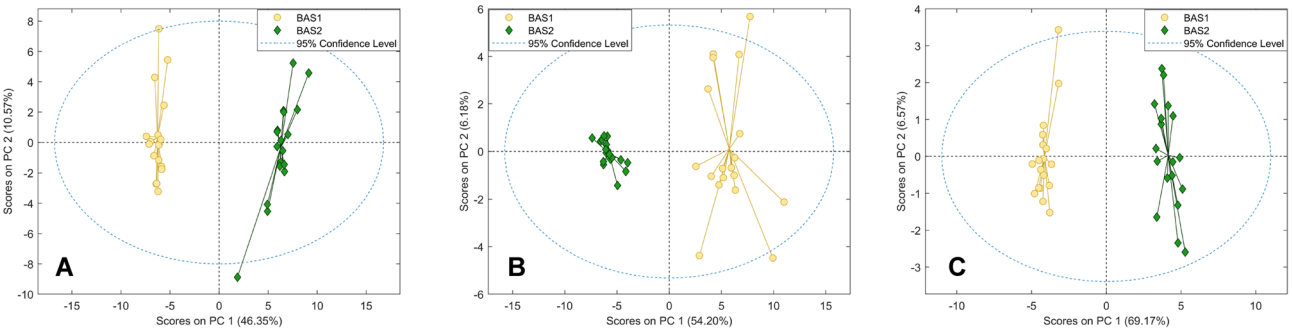

Fig. 13. PCA score plots (*Biogenic Amines*) of (**A**) Urine, (**B**) Stool, and (**C**) Serum *after* feature selection using the PLS_Toolbox software (Version 9.0; Eigenvector Research, Manson, WA).

Complex lipids

Prior to feature selection, no separation was observed between ***BAS1*** and ***BAS2*** for complex lipid urine samples (Fig. 10A). However, separation between ***BAS1*** and ***BAS2*** was observed along PC1 and PC2 for stool (Fig. 10B), and along PC1 for serum (Fig. 10C).

With feature selection, a clear separation was achieved between ***BAS1*** and ***BAS2*** along PC1 for all three biospecimens (Fig. 11A–C). It is noteworthy that more than three-quarters of the total variation was explained by PC1 for stool (76.7%) and serum (82.6%) samples. With FS-CR, 36 lipids in urine, 36 in stool, and 30 in serum were selected as significant metabolites describing differences between ***BAS1*** and ***BAS2***.

In urine, 25 lipids were positively correlated with ***BAS1***, and 11 lipids were correlated with ***BAS2*** (Supplementary Table 4).

In stool, 32 lipids were positively correlated with ***BAS1***, including eicosapentaenoic acid and various triglycerides, and four lipids were correlated with ***BAS2***, including margaric acid (Supplementary Table 5).

In serum, 14 lipids were positively correlated with ***BAS1***, including phosphatidylcholine 38:5 and phosphatidylcholine 40:7, and 16 lipids were correlated with BAS2, including sphingomyelin (d36:2) and several phosphatidylcholines (Supplementary Table 6).

Overall, the separation of ***BAS1*** and ***BAS2*** stool and serum in PCA space before feature selection indicates that the WD is altering the lipidome of the dogs. Separation of ***BAS1*** and ***BAS2*** for complex lipids in urine was only observed after feature selection. However, 36 urinary lipids were altered as a result of the WD, suggesting that the urinary lipidome of the dogs is also affected.

Biogenic amines

Prior to feature selection, there was significant overlap between ***BAS1*** and ***BAS2*** for urine (Fig. 12A). However, for stool (17.6%) and serum (11.8%) samples, there was a clear separation along PC2 (Fig. 12B and C). FS-CR identified 90 significant metabolites in urine, 68 significant metabolites in stool, and 26 significant metabolites in serum. After feature selection, ***BAS1*** and ***BAS2*** samples were clearly separated along PC1 for all biospecimens, accounting for approximately half of the total variance in the experimental data (Fig. 13).

In urine, 47 metabolites were positively correlated with ***BAS1***, including N-acetylmannosamine, threonic acid, nicotinamide, and dopamine (Supplementary Table 7). Additionally, 43 urinary metabolites were positively correlated with ***BAS2***, including N-methylphenylalanine, tartaric acid, and propoxyphene (Supplementary Table 7).

In stool, 51 metabolites were positively correlated with ***BAS1***, including O-acetylsalicylic acid, caffeic acid, and 3-pyridinemethanol, while 17 metabolites were correlated with ***BAS2***, including stachydrine and prochlorperazine (Supplementary Table 8).

In serum, 11 metabolites were positively correlated with ***BAS1***, including 4-aminobenzoic acid and L-histidinol, while 15 metabolites were correlated with ***BAS2***, including secnidazole, tartaric acid, and vanillin (Supplementary Table 9).

In summary, the separation of stool and serum samples between ***BAS1*** and ***BAS2*** before feature selection in PCA space suggests that the WD is altering the bioamine profile of the dogs. After feature selection, there was a clear separation of ***BAS1*** and ***BAS2*** for urine samples in PCA space, demonstrating that the WD is also altering the urinary biogenic amines profile of the dogs.

Discussion

The pleiotropic effects of SGLT-2 inhibitors and GLP-1 agonists hold the potential to target cardiorenal, hepatic and metabolic disorders using a disease model that replicates key features of ***MetS***. Previous experiments have primarily focused on obesity-related metabolic dysfunction when examining the effects of WDs in dogs. However, there is a lack of comprehensive studies on the biological and metabolic impacts of WDs independent of obesity. In both dogs and humans, obesity causes a redistribution of adipose tissue, leading to an increase in visceral fat compared to subcutaneous fat. This change in fat distribution is independently associated with the development of ***MetS***. This is significant as multiple reports, including analyses by Romero-Corral et al.[38] and Shi et al.[39] on large adult populations, have established that individuals with normal weight ***MetS*** are at an increased risk of cardiovascular diseases, metabolic dysregulation, and higher mortality rates compared to obese individuals with or without ***MetS***. In addition, most clinical investigations on the effectiveness of SGLT-2 inhibitors for cardiovascular and renal outcomes primarily include non-obese subjects[4,7,40–42]. Importantly, a recent study by Adamson et al.[43] demonstrated that in heart failure patients with reduced ejection fraction, the SGLT-2 inhibitor dapagliflozin effectively reduced the composite endpoint of worsening heart failure or cardiovascular death, regardless of the patient's baseline BMI. Collectively, these findings provide a compelling rationale for establishing a novel model of metabolic dysfunction that operates independently of obesity. Once established, this disease model will pave the way for in-depth studies on the pharmacodynamics of therapeutic drugs targeting cardiorenal metabolic health, including SGLT-2 inhibitors and GLP-1 agonists.

Our study maintained isocaloric conditions to isolate the effect of the diet's composition from obesity as a confounding factor. It builds on preliminary data from Lyu et al.[76], which showed a tendency towards elevated glucose concentrations in ten healthy Beagles under an isocaloric high-fat diet for six weeks. To the best of our knowledge, our research represents the first comprehensive characterization of the biological effects of a WD model, independent of obesity. By inducing ***MetS*** without causing weight gain, we have successfully developed a non-invasive, inducible, and potentially reversible preclinical model in just a few weeks. For ethical reasons and considerations related to animal welfare, it is important to emphasize that our objective was *not* to induce clinical symptoms of ***MetS*** in our study. Therefore, most of the observed changes reported herein remained within physiological limits. Overall, the WD was well tolerated with no reported adverse events during the study. Minor digestive issues appeared when transitioning from a regular diet to the WD, likely due to the absence of a proper weaning period between diets. However, these issues were resolved within a few days.

Hematological parameters typically remained within normal physiological limits, showing no clinically meaningful changes. The most notable variations were observed in metabolic parameters. Specifically, the WD induced a statistically significant increase in fasting blood glucose levels, approaching the upper physiological limit. This resulted in an overall increase of approximately 20% in blood glucose concentrations compared to baseline. Interestingly, this observation was accompanied by a trend towards an increase in peak insulin concentrations, which is consistent with previous literature in dogs[32,36] and indicative of a perturbation in insulin sensitivity that ultimately leads to insulin resistance[77]. The decrease in circulating glucagon concentrations may be symptomatic of a physiological feedback mechanism to maintain glucose homeostasis in response to increased fasting blood glucose[78].

Our dietary intervention also resulted in significant changes to serum chemistry parameters. These fluctuations, although still within physiological limits, demonstrate the ability of our model to greatly influence metabolism and homeostasis. Specifically, we observed a decrease in serum bicarbonate levels, which is in line with low-grade metabolic acidosis[79]. Our findings in dogs agree with previous data from the human literature. WDs are typically characterized by a high dietary acid load due to large amounts of animal protein and processed foods, which can exceed the kidneys' capacity to excrete the excess acid, leading to metabolic acidosis[80]. The concurrent increase in serum chloride concentrations reflects a state of hyperchloremic acidosis[81]. Overall, the association of hyperchloremic metabolic acidosis (with increased bicarbonate loss and a marked reduction in both phosphorus and potassium levels is consistent with some degree of renal tubular acidosis[82–84]. These findings are significant, as a recent meta-analysis, which included data from over 30,000 patients, found an association between metabolic acidosis, low bicarbonate levels, and features of ***MetS***[85]. Similarly, multiple studies have shown that low levels of potassium[86,87] and phosphorus[88,89] were associated with an increased risk for ***MetS*** in humans.

Consistent with the definition of ***MetS*** by the National Heart, Lung, and Blood Institute (NHLBI), our diet induced a significant elevation of SBP by approximately 10 mmHg. The increase in SBP appeared to be independent of any notable changes in renin and angiotensin peptides. Interestingly, SBP was not found to increase in a previous canine study focusing on obesity-related cardiac dysfunction and ***MetS***[90], again supporting our rationale for studying the effect of western diets independently of obesity. Our study also found mild increases in NT-proBNP, although mostly within the reference range. We suspect that the increase in circulating natriuretic peptides occurred secondarily to the increase in SBP, as previously reported in the literature[91,92], but it could also be indicative of cardiac stress[93]. Notably, some dogs showed NT-proBNP concentrations exceeding 900 pmol/L, a threshold commonly associated with structural heart disease in canines[94,95].

Total cholesterol increased by approximately 45% after ten weeks. Importantly, in line with the definition of ***MetS***, dogs fed the isocaloric WD model experienced a significant reduction in the AUC percentage of total HDL-cholesterol, along with an increase of the AUC percentage of LDL-cholesterol. Interestingly, upon examining the absolute value of each lipoprotein fraction, the absolute (untransformed) concentration of HDL-cholesterol increased after ***BAS1***. However, this increase was more modest compared to that of LDL-cholesterol. This suggests that the WD increased total cholesterol and caused a shift from HDL to LDL-cholesterol, which is also consistent with the development of ***MetS***. In addition to changes in total HDL and LDL-cholesterol, the WD also caused a significant decrease in the larger and less dense subfraction of HDL cholesterol (HDL 2a), with previous studies reporting a decreased risk of cardiovascular disease with higher levels of HDL2 cholesterol subfractions[96,97]. Consistent with these findings, the WD induced a significant increase in the small and dense subfractions of LDL cholesterol (LDL 3 and LDL 4), which are associated with a higher risk of atherosclerosis and stroke[98]. These changes occurred independently of any corresponding alterations in serum triglyceride concentrations, which is a variation from our preliminary data[44] showing an increase in serum triglycerides in 10 healthy dogs fed with a WD for seven weeks. Although we do not have a formal explanation for the discrepancy observed between the two studies, we hypothesize that differences in the age of the dogs (with dogs from our preliminary study being overall older, with a median age of 3 years) and the significant, although modest, increase in their body weight in Iennarella-Servantez et al.[44] could have contributed to the differences between studies. While surprising, this finding is also consistent with earlier research from Lahm Cardoso et al.[99] which showed a strong correlation between BCS and triglyceride levels in dogs, with values approaching the upper limit of 200 mg/dL in dogs with a BCS of 8 or above (classified as "overweight" or "obese" in our study).

Our results on redox status align with previous human studies[100–102]. Specifically, we observed significant increases in TOS and d-ROMs at ***BAS2***. In contrast, the effect on antioxidant markers was more nuanced and generally mild, with levels of CUPRAC, FRAP, TEAC, and Thiol remaining stable at ***BAS2***. This is in line with the variable impact of dietary fat on systemic antioxidative stress markers in dogs. Some studies have shown no effect of carbohydrate and fat concentrations on oxidative stress biomarkers[103], while others have reported an increase in antioxidant capacity, but no effect on oxidative stress markers[37].

Our study highlights the comprehensive changes in the metabolome induced by the WD, including biological pathways related to general metabolism, complex lipids, and biogenic amines. These observations underscore the potential relevance of this model in studying ***MetS*** and its associated health complications. Notably, all the metabolites detected in our study were classified according to MSI Level 2 standards[73]. The positive correlation of nicotinamide to the baseline diet (***BAS1***) in both general metabolism (urine) and biogenic amines (urine) suggests that dogs had lower amounts of this essential form of vitamin B3 after ten weeks of feeding with a WD (***BAS2***) compared to their standard diet. This is consistent with earlier findings from Qu et al.[104] reporting perturbations in nicotinamide metabolism in dogs fed a high-fat diet for twelve weeks. Nicotinamide plays a crucial role in various metabolic pathways, particularly in energy production and DNA repair[105,106]. Similarly, the positive correlation of glycerol to ***BAS2*** in general metabolomics (urine) indicates that glycerol concentrations were increased during feeding with the WD. Glycerol is a key component of triglycerides and is involved in energy metabolism, especially in lipid breakdown and synthesis[107]. This elevation is likely related to an increased metabolism of triglycerides caused by the WD, indicating a potential shift in lipid metabolism. The positive correlation of tartaric acid (2,3-dihydrobutanoic acid) with ***BAS2*** in multiple classes (general metabolomics in urine, biogenic amines in urine, and biogenic amines in serum) indicates that tartaric acid levels increased during the WD phase. These changes are possibly associated with the increased catabolism of the antioxidant ascorbic acid and accompany variations in oxidative stress markers highlighted above[108].

A greater diversity of fatty acids was correlated with ***BAS1***, especially in stool, indicating a wider range of fatty acid profiles in the baseline diet. This diversity is essential for energy production and cell membrane structure[109]. We suspect that the higher diversity of fatty acids in ***BAS1*** is due in part to the presence of more soluble dietary fiber, which is fermented by intestinal microbiota into short chain fatty acids[110]. After the WD diet, there was an increase in saturated fatty acids, specifically FA 17:0 in stool lipidomics and PC 18:0. High levels of saturated fatty acids have been linked to negative health outcomes, such as cardiovascular disease[111,112]. Furthermore, palmitoleic acid, an omega-7 monounsaturated fatty acid, showed a positive correlation with ***BAS2*** in stool general metabolomics. Palmitoleic acid (16:1n7) increases lipolysis, glucose uptake, and glucose utilization for energy production in white adipose cells[113,114]. The increase in saturated fatty acids, specifically FA 17:0 in ***BAS2***, could suggest a shift in lipid metabolism and/or be a result of the consumption of butter and ruminant fats[115]. While there is a decrease in fatty acid diversity and an increase in saturated fatty acids associated with ***BAS2***, it remains unclear whether these changes are related to ***MetS*** per se, or simply changes in stool composition caused by differences in diet composition.

In both general metabolomics (GC–MS) and LC–MS assays, several unidentified metabolites were detected. For GC–MS, this was due to spectral library matches failing to identify metabolites below the 800 threshold. Advanced data processing techniques, such as Parallel Factor Analysis, could be employed to deconvolve data and obtain cleaner spectra[116,117]. However, this would require a separate and dedicated study. Additionally, the bioamines assay detected several non-amine compounds due to its ability to detect compounds without an amine group. With LC–MS, the presence of unidentified metabolites could possibly be attributed to biotransformation of known metabolites, which involves the addition or removal of specific chemical moieties such as (de)-glycosylation, (de)-methylation, (de)-amination, and (de)-hydroxylation. These transformations often occur during metabolic processes[118]. To identify these metabolites, biotransformation analysis techniques and exploration of additional libraries and databases would be necessary. However, this is beyond the scope of this study. Despite the challenges in compound identification, the changes in metabolism observed across the three metabolomic assays are noteworthy. Additionally, several metabolites previously identified as both positively and negatively correlated with ***MetS*** in other studies, including nicotinamide, tryptophan metabolites, glycerol, and

tartaric acid, were found in the metabolomics analyses presented here[104–106,108,119]. This suggests that the WD is inducing metabolomic changes consistent with ***MetS*** in dogs.

This study presents several limitations that are worth mentioning. First, the experiment was limited in size and did not address the potential for reversibility of the model, specifically regarding the metabolic impacts of transitioning back to a standard diet. Due to the non-invasive nature of our model, this study was primarily descriptive and did not provide in-depth mechanistic insights into how WDs affect cardiovascular-kidney-metabolic health. The study also lacks some functional data, such as the time-dependent effects of the WD on intestinal permeability and fecal microbiome composition. This was partly deliberate, as those effects have been extensively characterized previously in the literature (e.g., Ref[32]). Previous studies published by our consortium in dogs[51–54] were conducted in the context of an activated RAAS. No elevation in PRA-S or angiotensin peptides was noted in the current study, which likely explains why many data points on aldosterone were below the lower limit of quantification, preventing statistical analysis of this biomarker. Additionally, our findings related to serum, urine and fecal metabolomics could be confounded by factors other than changes in diet composition, including differences in processing and ingredient composition between a commercial and a home-cooked diet. To minimize the impact of these potential confounding variables, we would need to conduct an experiment using two homemade diets with similar ingredients, while varying the proportions of fat, carbohydrates, and fiber to simulate the effect of a Western versus a standard diet on variables associated with ***MetS***. At last, determining whether metabolites are changing in response to altered metabolism or simply due to changes in dietary composition using untargeted metabolomics can be challenging. Therefore, mechanism-based hypothesis testing on the metabolome would require a targeted or semi-targeted approach that focuses on specific classes of metabolites.

In summary, our isocaloric WD, designed to mimic the NHANES diet, effectively replicated key characteristics of ***MetS.*** These included elevated BP, increased fasting glucose levels, and reduced HDL-cholesterol, all independent of abdominal obesity. Additionally, the WD induced an increase in natriuretic peptide levels, along with a mild state of metabolic acidosis and significant changes in the serum, urine, and fecal metabolome. Our findings underscore the utility of this model for investigating the metabolic effects of novel antidiabetic therapies in the context of obesity-independent ***MetS***, which will be presented in a separate manuscript. Furthermore, this research enables future translational studies that could have potential benefits for both human and veterinary medicine.

Ethical approval

Experimental procedures were approved by the Institutional Animal Care and Use Committee at Iowa State University (Protocol Number: 21-164). All methods were performed in accordance with the relevant guidelines and regulations at Iowa State University. The authors complied with ARRIVE guidelines in the completion of this study.

Data availability

Research data are available upon request. Please contact Jonathan P. Mochel (jpmochel@uga.edu).

Received: 8 April 2024; Accepted: 26 August 2024
Published online: 05 September 2024

References

1. Diabetes Prevention Program Research Group. Long-term effects of lifestyle intervention or metformin on diabetes development and microvascular complications over 15-year follow-up: The diabetes prevention program outcomes study. *Lancet Diabetes Endocrinol.* **3**(11), 866–875. https://doi.org/10.1016/S2213-8587(15)00291-0 (2015).
2. Centers for Disease Control and Prevention. National Diabetes Statistics Report website. https://www.cdc.gov/diabetes/data/statistics-report/index.html. Accessed 09 Dec 2023.
3. Birkeland, K. I. *et al.* How representative of a general type 2 diabetes population are patients included in cardiovascular outcome trials with SGLT-2 inhibitors? A large European observational study. *Diabetes Obes. Metab.* **21**(4), 968–974. https://doi.org/10.1111/dom.13612 (2019).
4. Butler, J. *et al.* EMPEROR-reduced trial committees and investigators. Empagliflozin and health-related quality of life outcomes in patients with heart failure with reduced ejection fraction: The EMPEROR-reduced trial. *Eur. Heart J.* **42**(13), 1203–1212. https://doi.org/10.1093/eurheartj/ehaa1007 (2021).
5. Inzucchi, S. E. *et al.* Are the cardiovascular and kidney benefits of empagliflozin influenced by baseline glucose-lowering therapy?. *Diabetes Obes. Metab.* **22**(4), 631–639. https://doi.org/10.1111/dom.13938 (2020).
6. Kosiborod, M. N. *et al.* Semaglutide in patients with heart failure with preserved ejection fraction and obesity. *N. Engl. J. Med.* **389**(12), 1069–1084. https://doi.org/10.1056/NEJMoa2306963 (2023).
7. McMurray, J. J. V. *et al.* The dapagliflozin and prevention of adverse-outcomes in heart failure (DAPA-HF) trial: Baseline characteristics. *Eur. J. Heart Fail.* **21**(11), 1402–1411. https://doi.org/10.1002/ejhf.1548 (2019).
8. Neal, B. *et al.* Canagliflozin and cardiovascular and renal events in type 2 diabetes. *N. Engl. J. Med.* **377**(7), 644–657. https://doi.org/10.1056/NEJMoa1611925 (2017).
9. Packer, M. *et al.* Design of a prospective patient-level pooled analysis of two parallel trials of empagliflozin in patients with established heart failure. *Eur. J. Heart Fail.* **22**(12), 2393–2398. https://doi.org/10.1002/ejhf.2065 (2020).
10. Persson, F. *et al.* Dapagliflozin is associated with lower risk of cardiovascular events and all-cause mortality in people with type 2 diabetes (CVD-REAL Nordic) when compared with dipeptidyl peptidase-4 inhibitor therapy: A multinational observational study. *Diabetes Obes. Metab.* **20**(2), 344–351. https://doi.org/10.1111/dom.13077 (2018).
11. Zinman, B. *et al.* Empagliflozin, cardiovascular outcomes, and mortality in type 2 diabetes. *N. Engl. J. Med.* **373**(22), 2117–2128. https://doi.org/10.1056/NEJMoa1504720 (2015).
12. Ndumele, C. E. *et al.* Cardiovascular-kidney-metabolic health: A presidential advisory from the American heart association. *Circulation* https://doi.org/10.1161/CIR.0000000000001184 (2023).

13. Grundy, S. M. *et al.* American heart association; national heart, lung, and blood institute diagnosis and management of the metabolic syndrome: An American heart association/national heart, lung, and blood institute scientific statement. *Circulation* **112**(17), 2735–2752. https://doi.org/10.1161/CIRCULATIONAHA.105.169404 (2005).
14. Newsome, P. N. & Ambery, P. Incretins (GLP-1 receptor agonists and dual/triple agonists) and the liver. *J. Hepatol.* **79**, 1557–1565. https://doi.org/10.1016/j.jhep.2023.07.033 (2023).
15. Jacob, J. A. Researchers turn to canine clinical trials to advance cancer therapies. *JAMA* **315**(15), 1550–1552. https://doi.org/10.1001/jama.2016.0082 (2016) (**PMID: 27027696**).
16. Seok, J. *et al.* Genomic responses in mouse models poorly mimic human inflammatory diseases. *Proc. Natl. Acad. Sci. U. S. A.* **110**(9), 3507–3512. https://doi.org/10.1073/pnas.1222878110 (2013).
17. Waring, M. J. *et al.* An analysis of the attrition of drug candidates from four major pharmaceutical companies. *Nat. Rev. Drug Discov.* **14**(7), 475–486. https://doi.org/10.1038/nrd4609 (2015).
18. Zushin, P. H., Mukherjee, S. & Wu, J. C. FDA modernization act 2.0: Transitioning beyond animal models with human cells, organoids, and AI/ML-based approaches. *J. Clin. Invest.* **133**(21), e175824. https://doi.org/10.1172/JCI175824 (2023).
19. Gilmore, K. M. & Greer, K. A. Why is the dog an ideal model for aging research?. *Exp. Gerontol.* **71**, 14–20. https://doi.org/10.1016/j.exger.2015.08.008 (2015) (**Epub 2015 Aug 29 PMID: 26325590**).
20. Gordon, I., Paoloni, M., Mazcko, C. & Khanna, C. The comparative oncology trials consortium: Using spontaneously occurring cancers in dogs to inform the cancer drug development pathway. *PLoS Med.* **6**(10), e1000161. https://doi.org/10.1371/journal.pmed.1000161 (2009).
21. Kaeberlein, M., Creevy, K. E. & Promislow, D. E. The dog aging project: Translational geroscience in companion animals. *Mamm. Genome* **27**(7–8), 279–288. https://doi.org/10.1007/s00335-016-9638-7 (2016).
22. Kopper, J. J. *et al.* Harnessing the biology of canine intestinal organoids to heighten understanding of inflammatory bowel disease pathogenesis and accelerate drug discovery: A one health approach. *Front. Toxicol.* **10**(3), 773953. https://doi.org/10.3389/ftox.2021.773953 (2021).
23. Masters, A. K. *et al.* Effects of short-term anti-inflammatory glucocorticoid treatment on clinicopathologic, echocardiographic, and hemodynamic variables in systemically healthy dogs. *Am. J. Vet. Res.* **79**(4), 411–423. https://doi.org/10.2460/ajvr.79.4.411 (2018) (**PMID: 29583045**).
24. Sebbag, L. & Mochel, J. P. An eye on the dog as the scientist's best friend for translational research in ophthalmology: Focus on the ocular surface. *Med. Res. Rev.* **40**(6), 2566–2604. https://doi.org/10.1002/med.21716 (2020).
25. Xenoulis, P. G. & Steiner, J. M. Lipid metabolism and hyperlipidemia in dogs. *Vet. J.* **183**(1), 12–21. https://doi.org/10.1016/j.tvjl.2008.10.011 (2010).
26. Kleinert, M. *et al.* Animal models of obesity and diabetes mellitus. *Nat. Rev. Endocrinol.* **14**(3), 140–162. https://doi.org/10.1038/nrendo.2017.161 (2018).
27. Yin, W. *et al.* Plasma lipid profiling across species for the identification of optimal animal models of human dyslipidemia. *J. Lipid Res.* **53**(1), 51–65. https://doi.org/10.1194/jlr.M019927 (2012).
28. Mochel, J. P. *et al.* Sacubitril/valsartan (LCZ696) significantly reduces aldosterone and increases cGMP circulating levels in a canine model of RAAS activation. *Eur. J. Pharm. Sci.* **1**(128), 103–111. https://doi.org/10.1016/j.ejps.2018.11.037 (2019).
29. Mochel, J. P. & Danhof, M. Chronobiology and pharmacologic modulation of the renin-angiotensin-aldosterone system in dogs: What have we learned?. *Rev. Physiol. Biochem. Pharmacol.* **169**, 43–69. https://doi.org/10.1007/112_2015_27 (2015) (**PMID: 26428686**).
30. Mochel, J. P. *et al.* Pharmacokinetic/pharmacodynamic modeling of renin-angiotensin aldosterone biomarkers following angiotensin-converting enzyme (ACE) inhibition therapy with benazepril in dogs. *Pharm. Res.* **32**(6), 1931–1946. https://doi.org/10.1007/s11095-014-1587-9 (2015).
31. Schneider, B. *et al.* Model-based reverse translation between veterinary and human medicine: The one health initiative. *CPT Pharmacometrics Syst. Pharmacol.* **7**(2), 65–68. https://doi.org/10.1002/psp4.12262 (2018).
32. Moinard, A. *et al.* Effects of high-fat diet at two energetic levels on fecal microbiota, colonic barrier, and metabolic parameters in dogs. *Front. Vet. Sci.* **25**(7), 566282. https://doi.org/10.3389/fvets.2020.566282 (2020).
33. Xue, J. *et al.* A protein- and fiber-rich diet with astaxanthin alleviates high-fat diet-induced obesity in beagles. *Front. Nutr.* **24**(9), 1019615. https://doi.org/10.3389/fnut.2022.1019615 (2022).
34. Peña, C. *et al.* Effects of low-fat high-fiber diet and mitratapide on body weight reduction, blood pressure and metabolic parameters in obese dogs. *J. Vet. Med. Sci.* **76**(9), 1305–1308. https://doi.org/10.1292/jvms.13-0475 (2014).
35. Sun, H. *et al.* Different diet energy levels alter body condition, glucolipid metabolism, fecal microbiota and metabolites in adult beagle dogs. *Metabolites* **13**(4), 554. https://doi.org/10.3390/metabo13040554 (2023).
36. Tvarijonaviciute, A. *et al.* Obesity-related metabolic dysfunction in dogs: A comparison with human metabolic syndrome. *BMC Vet. Res.* **28**(8), 147. https://doi.org/10.1186/1746-6148-8-147 (2012).
37. Vecchiato, C. G. *et al.* Fecal microbiota and inflammatory and antioxidant status of obese and lean dogs, and the effect of caloric restriction. *Front. Microbiol.* **12**(13), 1050474. https://doi.org/10.3389/fmicb.2022.1050474 (2023).
38. Romero-Corral, A. *et al.* Normal weight obesity: A risk factor for cardiometabolic dysregulation and cardiovascular mortality. *Eur. Heart J.* **31**(6), 737–746. https://doi.org/10.1093/eurheartj/ehp487 (2010).
39. Shi, T. H., Wang, B. & Natarajan, S. The influence of metabolic syndrome in predicting mortality risk among US adults: Importance of metabolic syndrome even in adults with normal weight. *Prev. Chronic Dis.* **21**(17), E36. https://doi.org/10.5888/pcd17.200020 (2020).
40. EMPA-KIDNEY Collaborative Group. Design, recruitment, and baseline characteristics of the EMPA-KIDNEY trial. *Nephrol. Dial. Transpl.* **37**(7), 1317–1329. https://doi.org/10.1093/ndt/gfac040 (2022).
41. Oyama, K. *et al.* Obesity and effects of dapagliflozin on cardiovascular and renal outcomes in patients with type 2 diabetes mellitus in the DECLARE-TIMI 58 trial. *Eur. Heart J.* **43**(31), 2958–2967. https://doi.org/10.1093/eurheartj/ehab530 (2022) (**PMID: 34427295**).
42. Wheeler, D. C. *et al.* The dapagliflozin and prevention of adverse outcomes in chronic kidney disease (DAPA-CKD) trial: baseline characteristics. *Nephrol. Dial. Transp.* **35**(10), 1700–1711. https://doi.org/10.1093/ndt/gfaa234 (2020).
43. Adamson, C. *et al.* Efficacy of dapagliflozin in heart failure with reduced ejection fraction according to body mass index. *Eur. J. Heart Fail.* **23**(10), 1662–1672. https://doi.org/10.1002/ejhf.2308 (2021).
44. Iennarella-Servantez, C. A. *et al.* Diet-induced clinical responsiveness of translational dog model for human western diet (WD)-related disease research. *J. Anim. Sci.* **99**(3), 58–59. https://doi.org/10.1093/jas/skab235.104 (2021).
45. German, A. J. *et al.* A simple, reliable tool for owners to assess the body condition of their dog or cat. *J. Nutr.* **136**(7 Suppl), 2031S-2033S. https://doi.org/10.1093/jn/136.7.2031S (2006) (**PMID: 16772488**).
46. National Health and Nutrition Examination Survey. (NHANES 2015–2016: Males and Females over 20 years). https://www.ars.usda.gov/northeast-area/beltsville-md-bhnrc/beltsville-human-nutrition-research-center/food-surveys-research-group/docs/temp-wweia-usual-intake-data-tables/.
47. National Research Council. *Nutrient Requirements of Dogs and Cats* (The National Academies Press, Washington, 2006).
48. Acierno, M. J. *et al.* ACVIM consensus statement: Guidelines for the identification, evaluation, and management of systemic hypertension in dogs and cats. *J. Vet. Intern. Med.* **32**(6), 1803–1822. https://doi.org/10.1111/jvim.15331 (2018).

49. Larner, C. D. High performance lipoprotein profiling for cardiovascular risk assessment. PhD thesis, Texas A&M University (2012).
50. Minamoto, T. *et al.* Altered lipoprotein profiles in cats with hepatic lipidosis. *J. Feline Med. Surg.* **21**(4), 363–372. https://doi.org/10.1177/1098612X18780060 (2019).
51. Schneider, B. K. *et al.* Breakthrough: A first-in-class virtual simulator for dose optimization of ACE inhibitors in translational cardiovascular medicine. *Sci. Rep.* **13**(1), 3300. https://doi.org/10.1038/s41598-023-30453-x (2023).
52. Sotillo, S. *et al.* Dose-response of benazepril on biomarkers of the classical and alternative pathways of the renin-angiotensin-aldosterone system in dogs. *Sci. Rep.* **13**(1), 2684. https://doi.org/10.1038/s41598-023-29771-x (2023).
53. Ward, J. L., Chou, Y. Y., Yuan, L., Dorman, K. S. & Mochel, J. P. Retrospective evaluation of a dose-dependent effect of angiotensin-converting enzyme inhibitors on long-term outcome in dogs with cardiac disease. *J. Vet. Intern. Med.* **35**(5), 2102–2111. https://doi.org/10.1111/jvim.16236 (2021).
54. Ward, J. L. *et al.* Circulating renin-angiotensin-aldosterone system activity in cats with systemic hypertension or cardiomyopathy. *J. Vet. Intern. Med.* **36**(3), 897–909. https://doi.org/10.1111/jvim.16401 (2022).
55. Domenig, O. *et al.* Neprilysin is a mediator of alternative renin-angiotensin-system activation in the Murine and human kidney. *Sci. Rep.* **21**(6), 33678. https://doi.org/10.1038/srep33678 (2016).
56. Guo, Z. *et al.* Measurement of equilibrium angiotensin II in the diagnosis of primary aldosteronism. *Clin. Chem.* **66**(3), 483–492. https://doi.org/10.1093/clinchem/hvaa001 (2020) (**PMID: 32068832**).
57. Zoufaly, A. *et al.* Human recombinant soluble ACE2 in severe COVID-19. *Lancet Respir. Med.* **8**(11), 1154–1158. https://doi.org/10.1016/S2213-2600(20)30418-5 (2020).
58. González-Arostegui, L. G., Muñoz-Prieto, A., Tvarijonaviciute, A., Cerón, J. J. & Rubio, C. P. Measurement of redox biomarkers in the whole blood and red blood cell lysates of dogs. *Antioxidants (Basel)* **11**(2), 424. https://doi.org/10.3390/antiox11020424 (2022).
59. Campos, C., Guzmán, R., López-Fernández, E. & Casado, A. Evaluation of the copper(II) reduction assay using bathocuproinedisulfonic acid disodium salt for the total antioxidant capacity assessment: The CUPRAC-BCS assay. *Anal. Biochem.* **392**(1), 37–44. https://doi.org/10.1016/j.ab.2009.05.024 (2009) (**Epub 2009 May 21 PMID: 19464250**).
60. Rubio, C. P. *et al.* Validation of three automated assays for total antioxidant capacity determination in canine serum samples. *J. Vet. Diagn. Invest.* **28**(6), 693–698. https://doi.org/10.1177/1040638716664939 (2016).
61. Benzie, I. F. & Strain, J. J. The ferric reducing ability of plasma (FRAP) as a measure of "antioxidant power": The FRAP assay. *Anal. Biochem.* **239**(1), 70–76. https://doi.org/10.1006/abio.1996.0292 (1996) (**PMID: 8660627**).
62. Arnao, M. B., Cano, A., Hernández-Ruiz, J., García-Cánovas, F. & Acosta, M. Inhibition by L-ascorbic acid and other antioxidants of the 2.2'-azino-bis(3-ethylbenzthiazoline-6-sulfonic acid) oxidation catalyzed by peroxidase: A new approach for determining total antioxidant status of foods. *Anal. Biochem.* **236**(2), 255–261. https://doi.org/10.1006/abio.1996.0164 (1996).
63. Da Costa, C. M., Dos Santos, R. C. C. & Lima, E. S. A simple automated procedure for thiol measurement in human serum samples. *J. Bras. Patol. Med. Lab.* **42**, 345–350. https://doi.org/10.1590/S1676-24442006000500006 (2006).
64. Tvarijonaviciute, A., Tecles, F., Caldin, M., Tasca, S. & Cerón, J. Validation of spectrophotometric assays for serum paraoxonase type-1 measurement in dogs. *Am. J. Vet. Res.* **73**(1), 34–41. https://doi.org/10.2460/ajvr.73.1.34 (2012) (**PMID: 22204286**).
65. Kapun, A. P., Salobir, J., Levart, A., Kotnik, T. & Svete, A. N. Oxidative stress markers in canine atopic dermatitis. *Res. Vet. Sci.* **92**(3), 469–470. https://doi.org/10.1016/j.rvsc.2011.04.014 (2012).
66. Verk, B., Nemec Svete, A., Salobir, J., Rezar, V. & Domanjko, P. A. Markers of oxidative stress in dogs with heart failure. *J. Vet. Diagn. Invest.* **29**(5), 636–644. https://doi.org/10.1177/1040638717711995 (2017).
67. Erel, O. A new automated colorimetric method for measuring total oxidant status. *Clin. Biochem.* **38**(12), 1103–1111. https://doi.org/10.1016/j.clinbiochem.2005.08.008 (2005) (**Epub 2005 Oct 7 PMID: 16214125**).
68. Tatzber, F., Griebenow, S., Wonisch, W. & Winkler, R. Dual method for the determination of peroxidase activity and total peroxides-iodide leads to a significant increase of peroxidase activity in human sera. *Anal. Biochem.* **316**(2), 147–153. https://doi.org/10.1016/s0003-2697(02)00652-8 (2003) (**PMID: 12711334**).
69. Alberti, A., Bolognini, L., Macciantelli, D. & Caratelli, M. The radical cation of N, N-diethyl-para-phenylendiamine: A possible indicator of oxidative stress in biological samples. *Res. Chem. Intermed.* **26**, 253–267. https://doi.org/10.1163/156856700X00769 (2000).
70. Rubio, C. P. *et al.* Stability of biomarkers of oxidative stress in canine serum. *Res. Vet. Sci.* **121**, 85–93. https://doi.org/10.1016/j.rvsc.2018.09.007 (2018).
71. Witko-Sarsat, V. *et al.* Advanced oxidation protein products as a novel marker of oxidative stress in uremia. *Kidney Int.* **49**(5), 1304–1313. https://doi.org/10.1038/ki.1996.186 (1996) (**PMID: 8731095**).
72. Matyash, V., Liebisch, G., Kurzchalia, T. V., Shevchenko, A. & Schwudke, D. Lipid extraction by methyl-tert-butyl ether for high-throughput lipidomics. *J. Lipid Res.* **49**(5), 1137–1146. https://doi.org/10.1194/jlr.D700041-JLR200 (2008).
73. Sumner, L. W. *et al.* Proposed minimum reporting standards for chemical analysis chemical analysis working group (CAWG) metabolomics standards initiative (MSI). *Metabolomics* **3**(3), 211–221. https://doi.org/10.1007/s11306-007-0082-2 (2007).
74. Adutwum, L. A., de la Mata, A. P., Bean, H. D., Hill, J. E. & Harynuk, J. J. Estimation of start and stop numbers for cluster resolution feature selection algorithm: An empirical approach using null distribution analysis of Fisher ratios. *Anal. Bioanal. Chem.* **409**(28), 6699–6708. https://doi.org/10.1007/s00216-017-0628-8 (2017).
75. Sinkov, N. A. & Harynuk, J. J. Cluster resolution: A metric for automated, objective and optimized feature selection in chemometric modeling. *Talanta* **83**(4), 1079–1087. https://doi.org/10.1016/j.talanta.2010.10.025 (2011).
76. Lyu, Y. *et al.* Differences in metabolic profiles of healthy dogs fed a high-fat vs. a high-starch diet. *Front. Vet. Sci.* **9**, 801863. https://doi.org/10.3389/fvets.2022.801863 (2022).
77. Cavaghan, M. K., Ehrmann, D. A. & Polonsky, K. S. Interactions between insulin resistance and insulin secretion in the development of glucose intolerance. *J. Clin. Invest.* **106**(3), 329–333. https://doi.org/10.1172/JCI10761 (2000).
78. Rix, I., Nexøe-Larsen, C., Bergmann, N. C., Lund, A. & Knop, F. K. Glucagon Physiology. In: Feingold, K. R., Anawalt, B., Blackman, M. R., Boyce, A., Chrousos, G., Corpas, E., de Herder, W. W., Dhatariya, K., Dungan, K., Hofland, J., Kalra, S., Kaltsas, G., Kapoor, N., Koch, C., Kopp, P., Korbonits, M., Kovacs, C. S., Kuohung, W., Laferrère, B., Levy, M., McGee, E. A., McLachlan, R., New, M., Purnell, J., Sahay, R., Shah, A. S., Singer, F., Sperling, M. A., Stratakis, C. A., Trence, D. L. & Wilson, D. P., (eds). South Dartmouth (MA): MDText.com, Inc. (2000).
79. Burger, M. & Schaller, D. J. Metabolic Acidosis. 2023 Jul 17. In: StatPearls [Internet]. Treasure Island (FL): StatPearls Publishing. PMID: 29489167 (2023).
80. Wieërs, M. L. A. J., Beynon-Cobb, B., Visser, W. J. & Attaye, I. Dietary acid load in health and disease. *Pflugers Arch.* **476**(4), 427–443. https://doi.org/10.1007/s00424-024-02910-7 (2024).
81. Sharma, S., Hashmi, M. F. & Aggarwal, S. Hyperchloremic Acidosis. In: StatPearls [Internet]. Treasure Island (FL): StatPearls Publishing (2023).
82. Bamgbola, O. F. Review of the pathophysiologic and clinical aspects of hypokalemia in children and young adults: An Update. *Curr. Treat Options Pediatr.* **8**(3), 96–114. https://doi.org/10.1007/s40746-022-00240-3 (2022).
83. Batlle, D. *et al.* Proximal renal tubular acidosis and hypophosphatemia induced by arginine. *Adv. Exp. Med. Biol.* **151**, 239–249. https://doi.org/10.1007/978-1-4684-4259-5_30 (1982) (**PMID: 6817609**).

84. Vasquez-Rios, G., Westrich, D. J. Jr., Philip, I., Edwards, J. C. & Shieh, S. Distal renal tubular acidosis and severe hypokalemia: A case report and review of the literature. *J. Med. Case Rep.* **13**(1), 103. https://doi.org/10.1186/s13256-019-2056-1 (2019).
85. Lambert, D. C., Kane, J., Slaton, A. & Abramowitz, M. K. Associations of metabolic syndrome and abdominal obesity with anion gap metabolic acidosis among US adults. *Kidney360* **3**(11), 1842–1851. https://doi.org/10.34067/KID.0002402022 (2022).
86. Stoian, M. & Stoica, V. The role of distubances of phosphate metabolism in metabolic syndrome. *Maedica (Bucur)* **9**(3), 255–260 (2014).
87. Sun, K. *et al.* Serum potassium level is associated with metabolic syndrome: A population-based study. *Clin. Nutr.* **33**(3), 521–527. https://doi.org/10.1016/j.clnu.2013.07.010 (2014).
88. Kalaitzidis, R., Tsimihodimos, V., Bairaktari, E., Siamopoulos, K. C. & Elisaf, M. Disturbances of phosphate metabolism: Another feature of metabolic syndrome. *Am. J. Kidney Dis.* **45**(5), 851–858. https://doi.org/10.1053/j.ajkd.2005.01.005 (2005) (**PMID: 15861350**).
89. Shimodaira, M., Okaniwa, S. & Nakayama, T. Reduced serum phosphorus levels were associated with metabolic syndrome in men but not in women: A cross-sectional study among the Japanese population. *Ann. Nutr. Metab.* **71**(3–4), 150–156. https://doi.org/10.1159/000480354 (2017).
90. Tropf, M., Nelson, O. L., Lee, P. M. & Weng, H. Y. Cardiac and metabolic variables in obese dogs. *J. Vet. Intern. Med.* **31**(4), 1000–1007. https://doi.org/10.1111/jvim.14775 (2017).
91. Hussain, A. *et al.* Association of NT-ProBNP, blood pressure, and cardiovascular events: The ARIC study. *J. Am. Coll. Cardiol.* **77**(5), 559–571. https://doi.org/10.1016/j.jacc.2020.11.063 (2021).
92. Jang, I. S., Yoon, W. K. & Choi, E. W. N-terminal pro-B-type natriuretic peptide levels in normotensive and hypertensive dogs with myxomatous mitral valve disease stage B. *Ir. Vet. J.* **76**(1), 3. https://doi.org/10.1186/s13620-023-00233-0 (2023).
93. Bayes-Genis, A. *et al.* Practical algorithms for early diagnosis of heart failure and heart stress using NT-proBNP: A clinical consensus statement from the heart failure association of the ESC. *Eur. J. Heart Fail.* https://doi.org/10.1002/ejhf.3036 (2023).
94. Singletary, G. E., Morris, N. A., Lynne O'Sullivan, M., Gordon, S. G. & Oyama, M. A. Prospective evaluation of NT-proBNP assay to detect occult dilated cardiomyopathy and predict survival in Doberman Pinschers. *J. Vet. Intern. Med.* **26**(6), 1330–1336. https://doi.org/10.1111/j.1939-1676.2012.1000.x (2012).
95. Wilshaw, J. *et al.* Accuracy of history, physical examination, cardiac biomarkers, and biochemical variables in identifying dogs with stage B2 degenerative mitral valve disease. *J. Vet. Intern. Med.* **35**(2), 755–770. https://doi.org/10.1111/jvim.16083 (2021).
96. Akinkuolie, A. O., Paynter, N. P., Padmanabhan, L. & Mora, S. High-density lipoprotein particle subclass heterogeneity and incident coronary heart disease. *Circ. Cardiovasc. Qual. Outcomes* **7**(1), 55–63. https://doi.org/10.1161/CIRCOUTCOMES.113.000675 (2014).
97. Superko, H. R. *et al.* High-density lipoprotein subclasses and their relationship to cardiovascular disease. *J. Clin. Lipidol.* **6**(6), 496–523. https://doi.org/10.1016/j.jacl.2012.03.001 (2012).
98. Duan, R. *et al.* Estimation of the LDL subclasses in ischemic stroke as a risk factor in a Chinese population. *BMC Neurol.* **20**(1), 414. https://doi.org/10.1186/s12883-020-01989-6 (2020).
99. Lahm Cardoso, J. M. *et al.* Blood pressure, serum glucose, cholesterol, and triglycerides in dogs with different body scores. *Vet. Med. Int.* **2016**, 8675283. https://doi.org/10.1155/2016/8675283 (2016).
100. Aleksandrova, K., Koelman, L. & Rodrigues, C. E. Dietary patterns and biomarkers of oxidative stress and inflammation: A systematic review of observational and intervention studies. *Redox Biol.* **42**, 101869. https://doi.org/10.1016/j.redox.2021.101869 (2021).
101. Boden, G. *et al.* Excessive caloric intake acutely causes oxidative stress, GLUT4 carbonylation, and insulin resistance in healthy men. *Sci. Transl. Med.* **7**(304), 304re7. https://doi.org/10.1126/scitranslmed.aac4765 (2015).
102. Matsuzawa-Nagata, N. *et al.* Increased oxidative stress precedes the onset of high-fat diet-induced insulin resistance and obesity. *Metabolism* **57**(8), 1071–1077. https://doi.org/10.1016/j.metabol.2008.03.010 (2008) (**PMID: 18640384**).
103. Chiofalo, B. *et al.* Effects of dietary protein and fat concentrations on hormonal and oxidative blood stress biomarkers in guide dogs during training. *J. Vet. Behav.* **37**, 86–92. https://doi.org/10.1016/j.jveb.2019.12.003 (2020).
104. Qu, W. *et al.* Profound perturbation in the metabolome of a canine obesity and metabolic disorder model. *Front. Endocrinol. (Lausanne)* **19**(13), 849060. https://doi.org/10.3389/fendo.2022.849060 (2022).
105. Amjad, S. *et al.* Role of NAD^+ in regulating cellular and metabolic signaling pathways. *Mol. Metab.* **49**, 101195. https://doi.org/10.1016/j.molmet.2021.101195 (2021).
106. Surjana, D., Halliday, G. M. & Damian, D. L. Role of nicotinamide in DNA damage, mutagenesis, and DNA repair. *J. Nucleic Acids.* **25**(2010), 157591. https://doi.org/10.4061/2010/157591 (2010).
107. Frühbeck, G., Méndez-Giménez, L., Fernández-Formoso, J. A., Fernández, S. & Rodríguez, A. Regulation of adipocyte lipolysis. *Nutr. Res. Rev.* **27**(1), 63–93. https://doi.org/10.1017/S095442241400002X (2014) (**Epub 2014 May 28 PMID: 24872083**).
108. Bánhegyi, G. & Loewus, F. A. Ascorbic acid catabolism: Breakdown pathways in animals and plants. In *Vitamin C, Function and Biochemistry in Animals and Plants* (eds Asard, H. *et al.*) 35 (Taylor & Francis, New York, 2004).
109. Hishikawa, D., Hashidate, T., Shimizu, T. & Shindou, H. Diversity and function of membrane glycerophospholipids generated by the remodeling pathway in mammalian cells. *J. Lipid Res.* **55**(5), 799–807. https://doi.org/10.1194/jlr.R046094 (2014).
110. Sivaprakasam, S., Prasad, P. D. & Singh, N. Benefits of short-chain fatty acids and their receptors in inflammation and carcinogenesis. *Pharmacol. Ther.* **164**, 144–151. https://doi.org/10.1016/j.pharmthera.2016.04.007 (2016).
111. Hooper, L. *et al.* Reduction in saturated fat intake for cardiovascular disease. *Cochrane Database Syst. Rev.* **5**(5), CD011737. https://doi.org/10.1002/14651858.CD011737.pub2 (2020).
112. Siri-Tarino, P. W., Sun, Q., Hu, F. B. & Krauss, R. M. Saturated fat, carbohydrate, and cardiovascular disease. *Am. J. Clin. Nutr.* **91**(3), 502–509. https://doi.org/10.3945/ajcn.2008.26285 (2010).
113. Bolsoni-Lopes, A. *et al.* Palmitoleic acid (n-7) increases white adipocytes GLUT4 content and glucose uptake in association with AMPK activation. *Lipids Health Dis.* **20**(13), 199. https://doi.org/10.1186/1476-511X-13-199 (2014).
114. Cruz, M. M. *et al.* Palmitoleic acid (16:1n7) increases oxygen consumption, fatty acid oxidation and ATP content in white adipocytes. *Lipids Health Dis.* **17**(1), 55. https://doi.org/10.1186/s12944-018-0710-z (2018).
115. Alves, S. P., Marcelino, C., Portugal, P. V. & Bessa, R. J. Short communication: The nature of heptadecenoic acid in ruminant fats. *J. Dairy Sci.* **89**(1), 170–173. https://doi.org/10.3168/jds.S0022-0302(06)72081-1 (2006) (**PMID: 16357280**).
116. Amigo, J. M., Skov, T., Bro, R., Coello, J. & Maspoch, S. Solving GC-MS problems with PARAFAC2. *TrAC Trends Anal. Chem.* **27**, 714–725. https://doi.org/10.1016/j.trac.2008.05.011 (2008).
117. Giebelhaus, R. T., Sorochan Armstrong, M. D., de la Mata, A. P. & Harynuk, J. J. Untargeted region of interest selection for gas chromatography–mass spectrometry data using a pseudo F-ratio moving window. *J. Chromatogr. A* **1682**, 463499. https://doi.org/10.1016/j.chroma.2022.463499 (2022).
118. Giebelhaus, R. T., Erland, L. A. E. & Murch, S. J. HormonomicsDB: A novel workflow for the untargeted analysis of plant growth regulators and hormones. *F1000Research* **11**, 119 (2022).
119. Monnerie, S. *et al.* Metabolomic and lipidomic signatures of metabolic syndrome and its physiological components in adults: A systematic review. *Sci. Rep.* **10**(1), 669. https://doi.org/10.1038/s41598-019-56909-7 (2020).
120. Kadowaki, T. *et al.* Interconnection between cardiovascular, renal and metabolic disorders: A narrative review with a focus on Japan. *Diabetes Obes. Metab.* **24**(12), 2283–2296. https://doi.org/10.1111/dom.14829 (2022).

121. National Heart, Lung, and Blood Institute (NHLBI). What is metabolic syndrome? https://www.nhlbi.nih.gov/health/metabolic-syndrome#:~:text=Metabolic%20syndrome%20is%20a%20group,also%20called%20insulin%20resistance%20syndrome. Last 18 May 2022.
122. R: A language and environment for statistical computing. R Foundation for Statistical Computing, Vienna, Austria. https://www.R-project.org/
123. Rubio, C. P., Martinez-Subiela, S., Hernández-Ruiz, J., Tvarijonaviciute, A. & Ceron, J. J. Analytical validation of an automated assay for ferric-reducing ability of plasma in dog serum. *J. Vet. Diagn. Invest.* **29**(4), 574–578. https://doi.org/10.1177/1040638717693883 (2017).
124. Johnson, M. C. Hyperlipidemia disorders in dogs. *Compend. Contin. Educat. Pract. Vet.* **27**, 361–364 (2005).
125. Littman, M. P. Spontaneous systemic hypertension in 24 cats. *J. Vet. Intern. Med.* **8**(2), 79–86. https://doi.org/10.1111/j.1939-1676.1994.tb03202.x (1994). PMID: 8046680.
126. Jocelyn, P. C. Spectrophotometric assay of thiols. *Methods Enzymol.* **143**, 44–67. https://doi.org/10.1016/0076-6879(87)43013-9 (1987). PMID: 3657559.

Author contributions

J.P.M.: concept and design of the study, analysis and interpretation of the data, manuscript preparation and revisions; J.L.W.: concept and design of the study, data acquisition, manuscript revisions; T.B.: data analysis and interpretation, manuscript revisions; D.K.: data analysis and interpretation, manuscript revisions; M.M.M.: data acquisition, manuscript revisions; C.Z.: concept and design of the study, funding; E.G.: concept and design of the study, funding; R.T.G.: data analysis and interpretation, manuscript revisions; P.d.l.M.: data analysis and interpretation, manuscript revisions; C.A.I.: concept of the study (NHANES WD); A.B.: concept and design of the study, manuscript revisions; S.L.N.: data analysis and interpretation, manuscript revisions; J.J.H.: data analysis and interpretation, manuscript revisions; J.S.: data analysis and interpretation, manuscript revisions; A.T.: data interpretation, manuscript revisions; J.J.C.: data analysis and interpretation, manuscript revisions; A.B.M.: data acquisition, manuscript revisions; F.Z.: data interpretation, manuscript revisions; N.S.: data interpretation, manuscript revisions; K.A.: concept and design of the study, manuscript revisions.

Funding

This study was sponsored by Ceva Sante Animale, 33500 Libourne (France).

Competing interests

Mochel, Ward, Zannad, Sattar, and Allenspach act as consultants for Ceva Sante Animale. Blondel, Zemirline, and Guillot are employees of Ceva Sante Animale. All other authors do not have a conflict of interest.

Additional information

Supplementary Information The online version contains supplementary material available at https://doi.org/10.1038/s41598-024-71202-y.

Correspondence and requests for materials should be addressed to J.P.M.